Electronic Supplementary Material (ESI) for Catalysis Science & Technology.
This journal is © The Royal Society of Chemistry 2022

Electronic Supporting Information:

Robust Palladium Catalysts on Nickel Foam for Highly Efficient Hydrogenations

Azina Rahmani,[a] Taylor M. Currie,[a] Lorianne R. Shultz,[a] Jacob T. Bryant,[a] Melanie J. Beazley,[a] Fernando J. Uribe-Romo,[a] Laurene Tetard,[b],[c] Nicholas G. Rudawski,[d] Shaohua Xie,[e] Fudong Liu,[c],[e],[f] Ting-Hsuan Wang,[g] Tiow-Gan Ong,[g] Lei Zhai,[a],[c] Titel Jurca*[a],[c],[f]

[a] *Department of Chemistry, University of Central Florida, Orlando, Florida, USA, 32816; Email- titel.jurca@ucf.edu*
[b] *Department of Physics, University of Central Florida, Orlando, Florida, USA, 32816*
[c] *NanoScience and Technology Center (NSTC), University of Central Florida, Orlando, Florida, USA, 32826*
[d] *Herbert Wertheim College of Engineering Research Service Centers, University of Florida, Gainesville, FL, USA, 32611*
[e] *Department of Civil, Environmental, and Construction Engineering, University of Central Florida, Orlando, Florida, USA, 32816*
[f] *Renewable Energy and Chemical Transformations Faculty Cluster (REACT), University of Central Florida, Orlando, Florida, USA, 32816*
[g] *Institute of Chemistry, Academia Sinica, Taipei, Taiwan, ROC*

General Methods

All materials were handled under ambient lab atmosphere. Nickel foam was purchased from MTI Corporation as 1.6 mm thick roll of 1000 mm x 300 mm dimension, with >99.9 wt% Ni purity. Absolute ethanol and hydrochloric acid were purchased from Fisher Chemical. Palladium acetate and anthracene were purchased from Acros Organics. Nitrobenzene, N,N-Dimethyl-4-nitroaniline, 4-Methyl-3-nitroaniline, 4-nitrostyrene, 4-vinylphenol (stabilized with propylene glycol), 2,4,6-trimethylstyrene, 4-methylstyrene, 4-bromostyrene, and $CDCl_3$ were purchased from Alfa Aesar. E-ethylnitrobenzene, 4-nitrophenol, 3-nitroaniline, 2-methyl-5-nitroaniline, 1-iodo-2-nitrobenzene, 4-chlorostyrene, and 4-(trifluoromethyl)styrene were purchased from Tokyo Chemical Industry (TCI). Dopamine hydrochloride, 4,5-dimethyl-2-nitroaniline, 4-nitro-1-naphtylamine, and styrene were purchased from Millipore Sigma. All chemicals were used as received without further purification. Nuclear magnetic resonance (NMR) spectroscopy measurements were conducted on a Bruker Avance III HD 400 MHz spectrometer, and the data analyzed using Mestrelab Research MestReNova version 14.2.3-29241 software.

Materials Synthesis: Nickel foam was cut into rectangular blocks (24 mm L, 12 mm W, 1.6 mm thickness, and weight of ~ 0.1 g) and cleaned by ultrasonication in hydrochloric acid solution and rinsing thoroughly with DI water. Next, the foams were dried in an oven (150 ˚C). Cleaned Ni foams (1.7 g) were immersed in an aqueous solution of dopamine hydrochloride (1 g dopamine hydrochloride in 100 mL DI water) at 150 °C under stirring (in a sealed 250 mL heavy wall high pressure flask). After 4 hours, the foams were removed from the reaction flask and rinsed with DI water. In the subsequent step, the polydopamine coated foams were immersed in the solution of metal precursor, palladium acetate (0.3 g palladium acetate, 25 mL ethanol, and 75 mL DIW) at 150 °C under stirring (150 rpm) to induce deposition of Pd on the foam (in a sealed 250 mL heavy wall high pressure flask). After 70 hours, the foams were washed with DI water and dried in the oven at 150 °C overnight. ALD was performed using a CTECHnano Play Series thermal ALD reactor at a chamber temperature of 160°C, and inlet and outlet temperatures of 100°C. The precursors, trimethylaluminum (TMA) and water (H_2O), were alternatively pulsed for 250 msec, followed by a 1 s residence time, and 14 s purge each. This recipe was repeated for 22 cycles to deposit an estimated thickness of 2 nm of Al_2O_3. The materials were annealed at 400 °C for 1 hour in air (at heating rate of 5 ◦C/min). ***Pd/Ni*** *and* ***Pd-D/Ni*** *were prepared under similar conditions, but without the respective steps associated with the missing component. These materials and their preparation and characterization will be elaborated upon in a forthcoming, comprehensive study.*

pXRD: In house laboratory X-ray diffraction was collected using a Rigaku MiniFlex 600 θ-2θ diffractometer in Bragg-Brentano geometry with a 300 mm goniometer diameter, Ni-filtered CuKα radiation (λ = 1.5418 Å), at 600 W power (40 kV, 15 mA), equipped with a high-resolution D/tex 250 detector, 5.0º incident and receiving Soller slits, a 0.625º divergent slit, a 1.25º scattering slit, a 0.3 mm receiving slit, a Ni-CuKβ filter, and an antiscattering blade. Samples were analyzed from 5 to 80 2θ-degrees with 0.02º per step and a scan rate of 1.0 2θ-degrees min^{-1}. Samples were prepared by placing the coated foams on an aluminum sample holder and centered for uniformity between samples.

XPS: X-ray photoelectron spectroscopy data was obtained using a Thermo Scientific ESCALAB XI^+ X-ray Photoelectron Spectrometer with an Al Kα X-ray source (1486.67 eV) and spot size of 650 µm. The samples were loaded on carbon tape and binding energies acquired were calibrated to carbon 1s sp^3 at 284.8 eV. A pass energy of 20.0 eV was used with energy step sizes of 0.05 eV and 50 ms dwell times for the high-resolution spectra and step sizes of 0.5 eV with 20 ms dwell times for the survey scans. Survey spectra and high-resolution spectra are comprised of an average of three and eight scans respectively. Peak fitting was completed through Thermo Scientific's Avantage Data System and XPSPeak41.

ICP-MS: A solid 54.5 mg sample of **Pd-D/Ni@Al_2O_3** was agitated overnight at room temperature in 4% nitric acid (trace metal grade; Fisher Scientific) until complete dissolution. The solution was filtered with a 0.45 µm pore size polypropylene membrane filter and analyzed by inductively coupled plasma mass spectrometry (ICP-MS). Dissolved Pd concentrations were measured using a Thermo Fisher Scientific iCap Qc ICP-MS with QCell technology and operated in kinetic energy discrimination (KED) mode of analysis with helium as the collision gas. Calibration, internal, and quality control standards (Inorganic Ventures) were prepared in 2% trace metal grade nitric acid (Fisher Scientific). Bismuth and rhodium were used as internal references.

SEM & TEM: Elemental mapping was performed using the scanning electron microscope (SEM) column of a Helios G4 PFIB CXe dual beam instrument equipped with an EDAX Octane Elite SDD energy dispersive spectroscopy (EDS) system (70 mm2 active area); the SEM voltage was 10 kV with a beam current of 1.3 nA while the EDS detector dispersion was 5 eV/channel with an amp time of 0.96 us. All elemental maps shown are net intensity, meaning potential peak overlaps and background signals are accounted for and/or removed. Conventional and high-angle annular dark-field scanning transmission electron microscopy (HAADF-STEM) was performed using an FEI Themis Z scanning/transmission electron microscope (third and fifth order Cs probe corrected) operating at 200 kV. Conventional images were acquired using a

bottom-mounted Ceta camera and HAADF-STEM images were collected using a Fischione Instruments Model 3000 HAADF-STEM detector. Elemental mapping was performed while operating in scanning mode with ~300 pA probe current using a SuperX windowless SDD energy dispersive spectroscopy system with ~0.7 sr solid angle of collection. TEM specimens were prepared by ultrasonicating a scraped residue from the surface of **Pd-D/Ni@Al_2O_3** in a few mL of methanol and then drop casting 1 or 2 drops of solution onto a Cu grid with a lacey C support film; the grids were then allowed to dry for several minutes while suspended over a warm hotplate (~100 °C) using locking tweezers to facilitate evaporation of the solvent. Immediately prior to performing TEM, the grids were plasma cleaned for ~20 s using a Fischione Instruments Model 1020 plasma cleaner.

AFM: AFM topography images were collected in tapping mode on a nanoIR2 AFM system (Bruker) with standard tapping mode tips (k=42 N/m). The cantilever was excited at their first resonance. Several regions of the foams were imaged to identify representative area. Image processing to extract line profiles and reconstruct a 3D display of the topography was obtained with Gwyddion.[1]

Surface Area: BET surface area and pore size distribution were determined on a Quantachrome Autosorb-iQ physisorption chemisorption instrument. Prior to testing, the samples were outgassed at 300 ^oC for 1 h to remove all adsorb molecules from the surface, and the nitrogen adsorption–desorption isotherm was measured using pressure intervals of $0 < P/P_0 < 1$ with 20 adsorption steps and 20 desorption steps. BET surface areas were calculated by using adsorption point at P/P_0 of 0.3. The non-local density functional theory (DFT) method was used to determine pore size distribution of the samples.

General batch catalytic reaction protocol: Catalytic hydrogenations were performed in a 25 mL Büchiglasuster tinyclave glass insert reactor (charged with 1 mmol substrate, 59.9 ± 1.5 mg catalyst), and 5 mL of absolute ethanol (no effort to dry or avoid ambient moisture, ~50%, contamination) as solvent. The reactor was pressurized with ultrahigh purity H_2 gas supplied by Airgas and then heated in an oil bath to the specified temperature (main manuscript, Scheme 1). When the reaction was complete, the reactor was cooled down to room temperature/22 °C and depressurized. The catalyst was physically separated for the next run with tweezers, and ethanol in the product mixture was removed under reduced pressure. The product was analyzed by proton nuclear magnetic resonance spectroscopy (^{1}H NMR) in $CDCl_3$.

Flow reaction protocol: A 7.7 mm inner diameter by 970 mm stainless steel tube was filled with 40 x stacked catalyst discs (**Pd-D/Ni@Al_2O_3** ~800 mg). All components were connected by 1.6 mm outer diameter PTFE tubing from Kimble® and with PEEK fitting/connectors/valves. The reactor was wrapped with heating tape controlled by a J-KEM Scientific Model 210 heater and proprietary software. Two Fisher Scientific Model 100 programmable syringe pumps were used. Syringe Pump 1, containing the substrate diluted in 40 mL of absolute ethanol was additionally wrapped in a syringe heater from Braintree Scientific and matched in temperature to the reactor bed. Syringe Pump 2 containing absolute ethanol was used to flush the system before and after each use. A switchable 4-junction connector with 3-way flow was used to integrate the two pumps and H_2 gas inlet, and served as the mixer for incoming streams. The product stream flows into a capped collection bottle in which H_2 gas was allowed to vent. A valve above the sample container was used to collect product aliquots at various timepoints. Ethanol in the product mixture was removed under reduced pressure. The product was analysed by proton nuclear magnetic resonance spectroscopy (^{1}H NMR) in $CDCl_3$.To regenerate the catalyst, the tube containing the discs of catalyst was disconnected from the system and annealed under ambient atmosphere at 400 °C for 1 hour (at the rate of 5 °C/min).

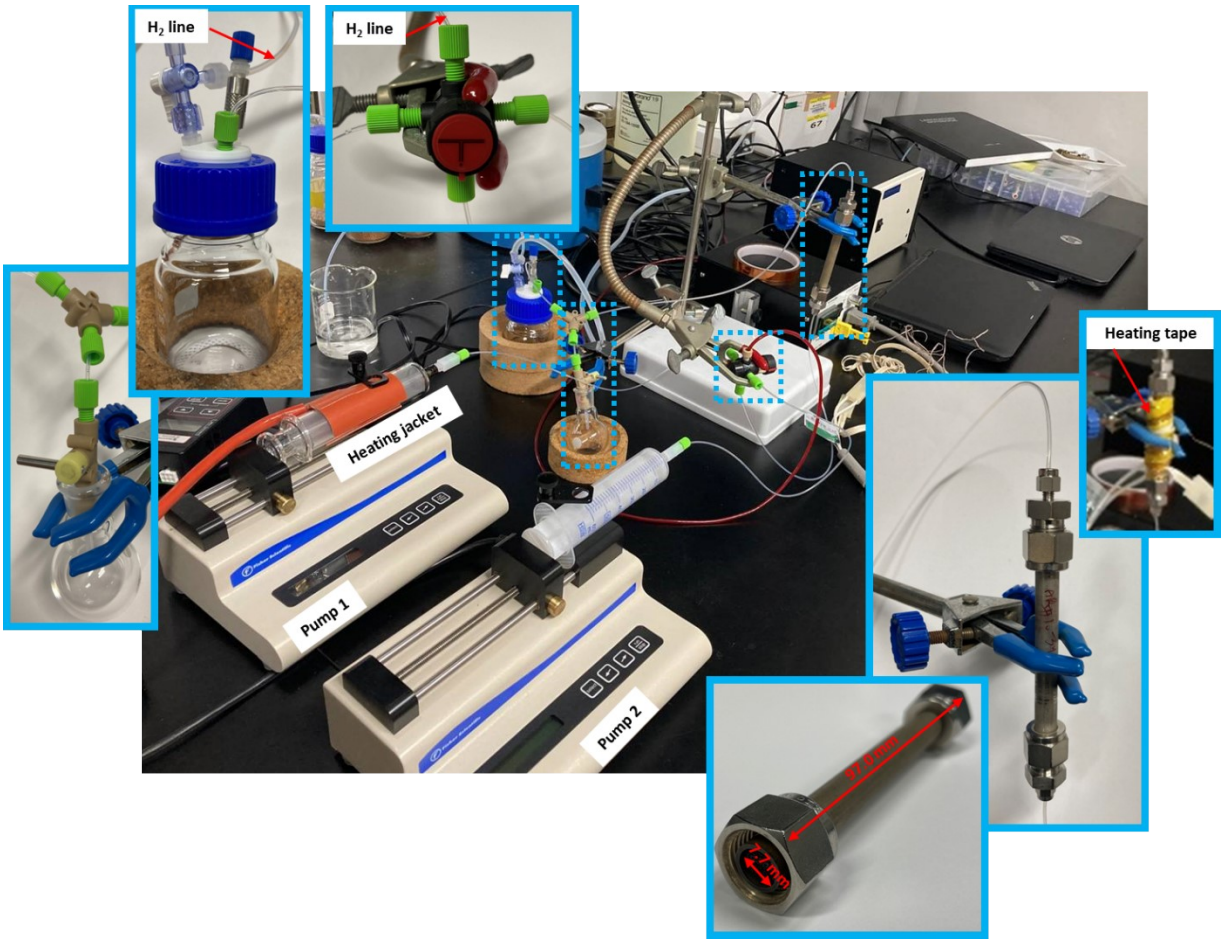

Fig. S1 Photograph of benchtop continuous flow catalysis setup. See Fig 3A in manuscript for schematic.

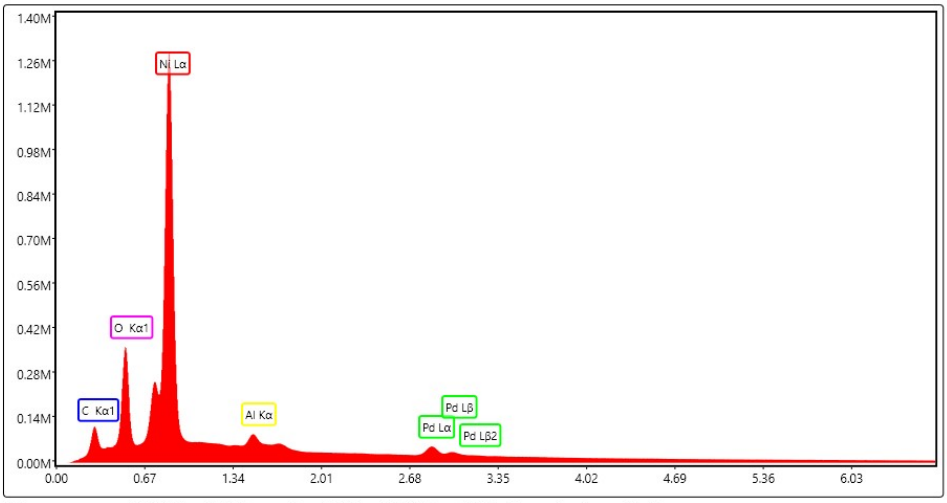

Fig. S2 Energy dispersive x-ray spectrum of **Pd-D/Ni@Al_2O_3** as highlighted in main manuscript, Fig. 2C. (*x axis = KeV*)

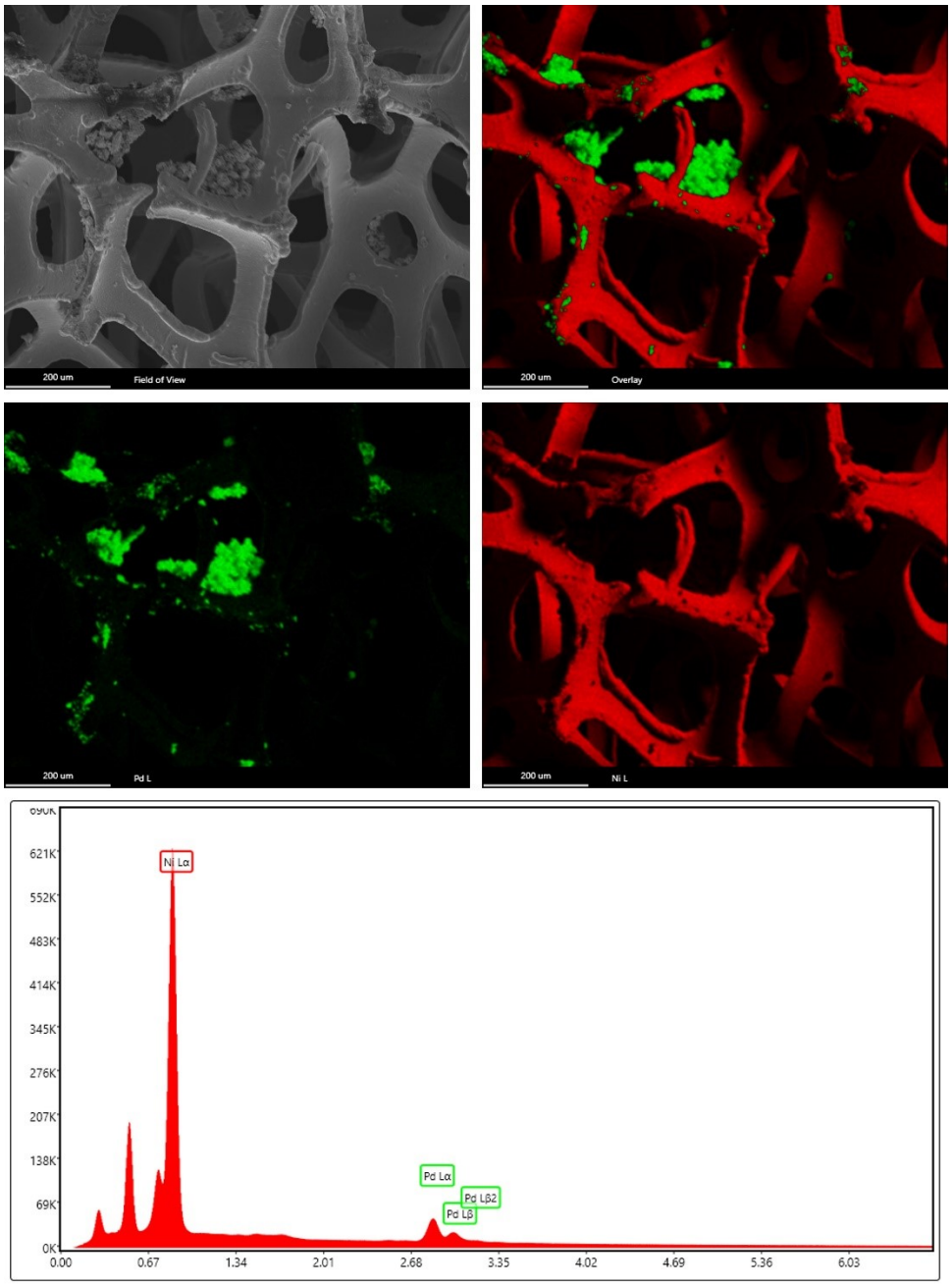

Fig. S3 SEM Micrograph and corresponding EDS of **Pd/Ni**. (*x axis = KeV*)

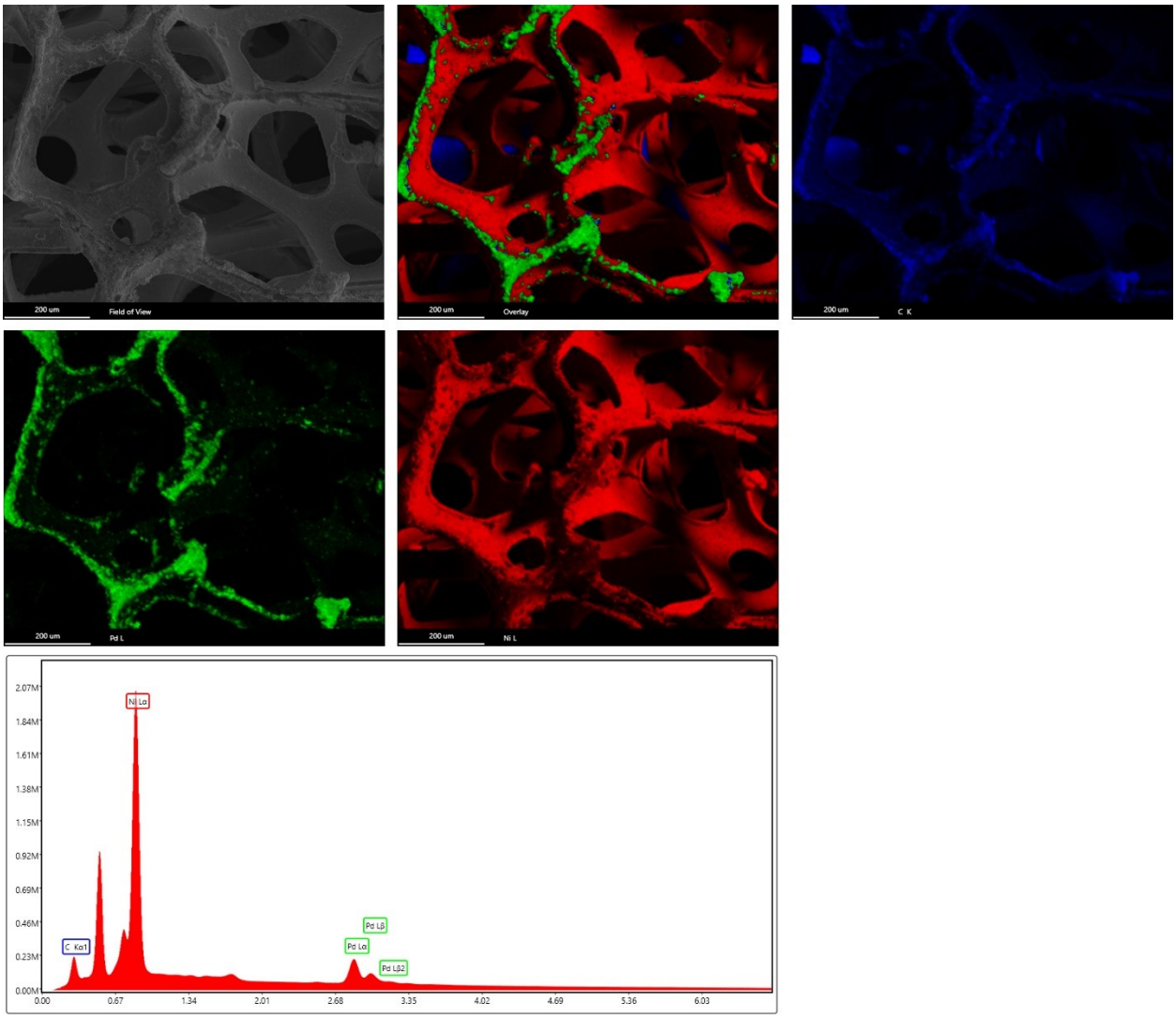

Fig. S4 SEM Micrograph and corresponding EDS of **Pd-D/Ni**. (*x axis = KeV*)

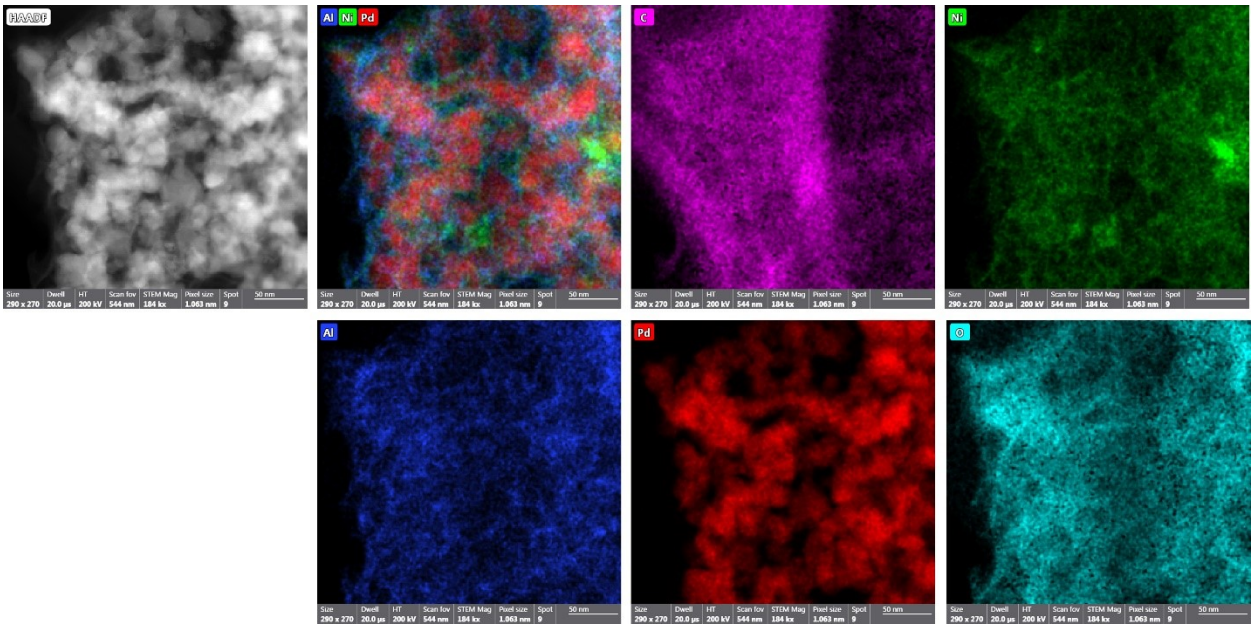

Fig. S5 HAADF-STEM micrograph and composite EDS elemental mapping of **Pd-D/Ni@Al_2O_3** scraped off Ni foam surface – as highlighted in the main manuscript, Fig. 2E.

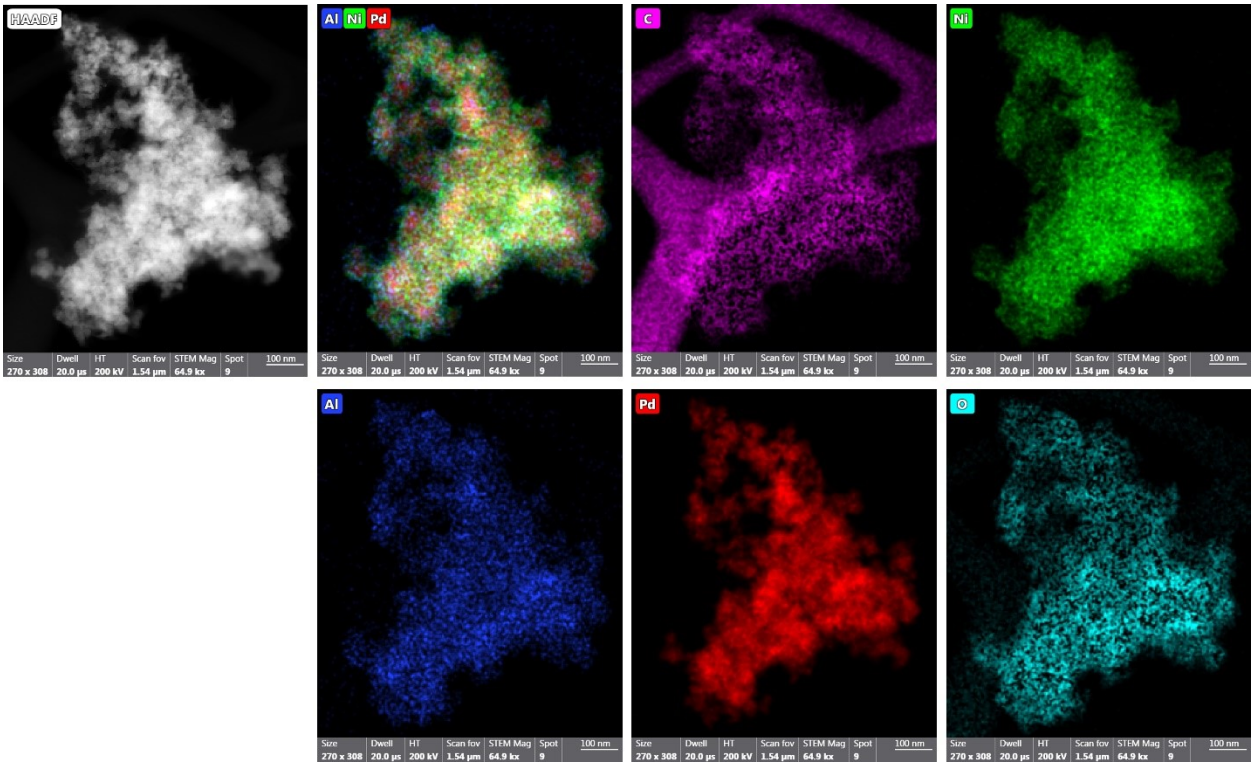

Fig. S6 Additional HAADF-STEM micrograph and composite EDS elemental mapping of **Pd-D/Ni@Al_2O_3** scraped off Ni foam surface – higher intensity Ni signal commensurate with imaging the back side of the flake.

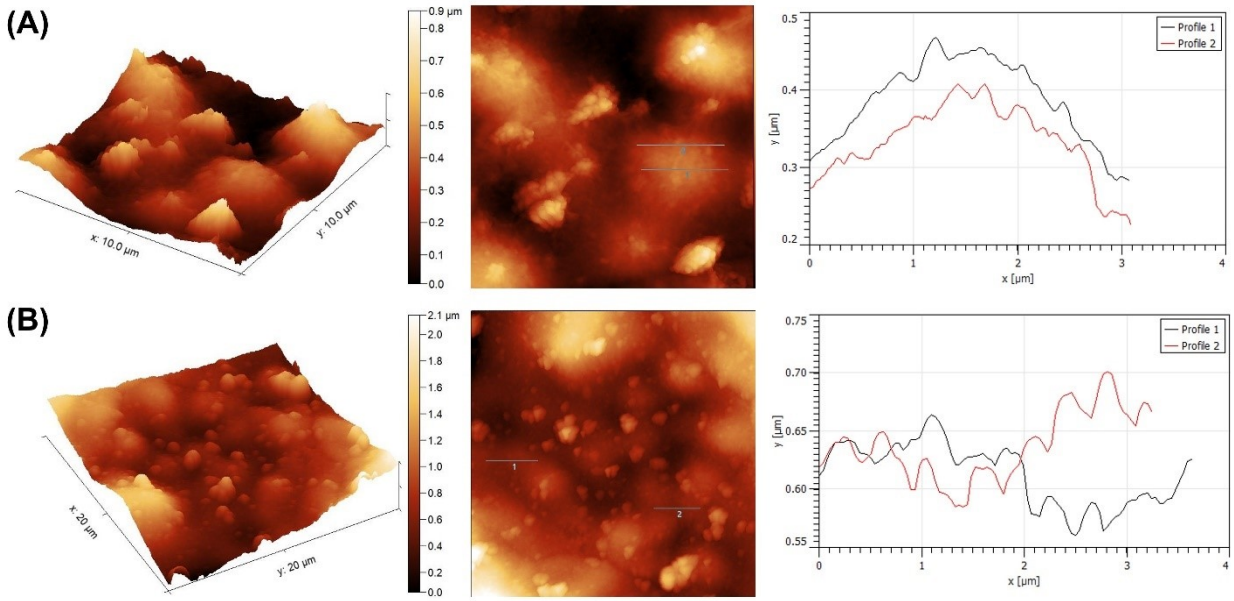

Fig. S7 (A,B) AFM micrographs and accompanying height profiles for two separate regions of **Pd-D/Ni@Al_2O_3**.

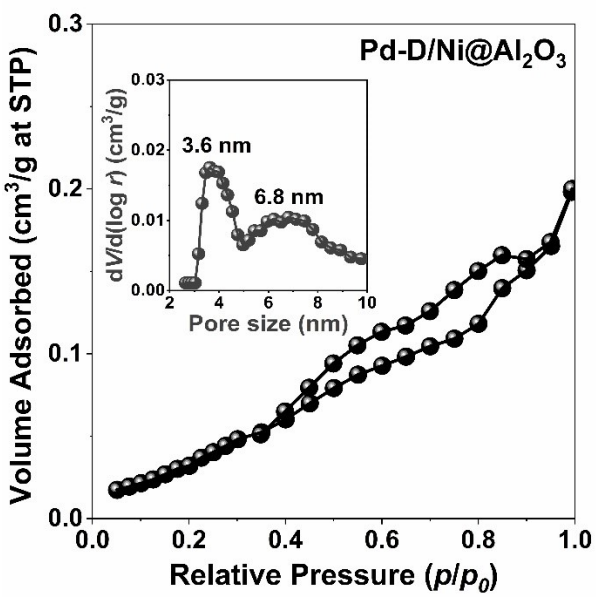

Fig. S8 BET measurement of **Pd-D/Ni@Al_2O_3**. *Inset = pore size distribution.*

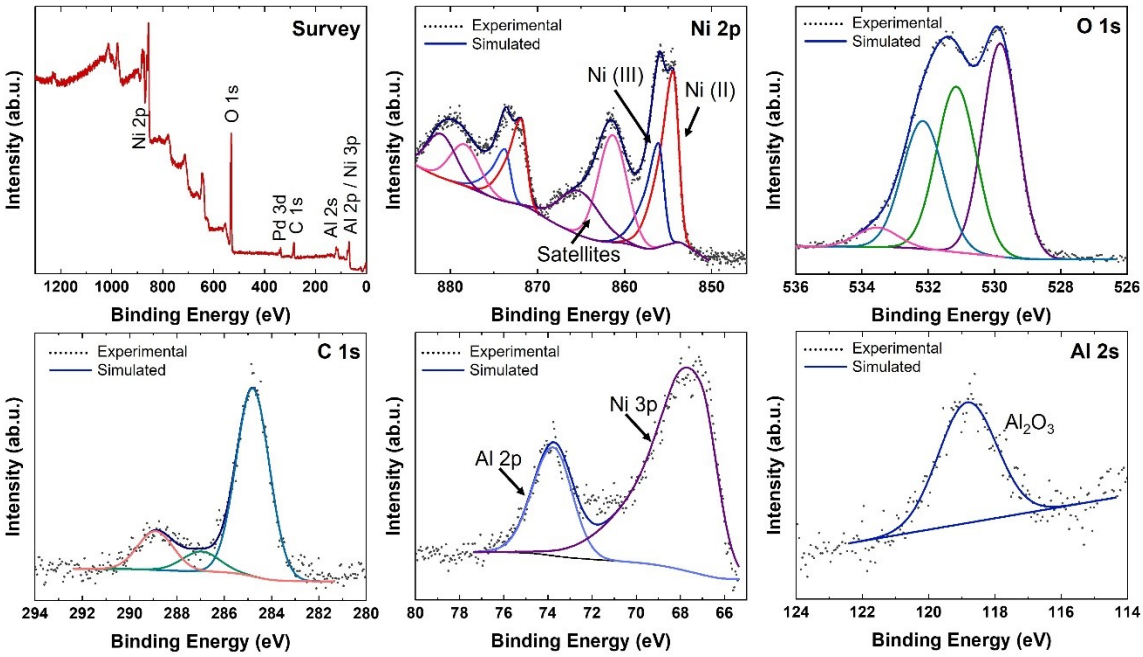

Fig. S9 XPS spectra of **Pd-D/Ni@Al_2O_3** (*top left*) survey scan; (*top middle*) nickel region fitted to two peaks corresponding to Ni(II) and Ni(III); (*top right*) oxygen region fitted to four peaks. *The three centered at 529.8, 531.2, and 532.2 eV are likely lattice oxygen for the nickel-, palladium-, and aluminum-oxides, and the peak at 532.16 eV is likely adsorbed water*; (*bottom left*) carbon region fitted to peaks characteristic of C-C/C=C, C-O-C, and C-O=C from lowest to highest binding energy; (*bottom middle*) shows the region which includes Al 2p and Ni 3p; (*bottom right*) Al 2s region fitted to one peak for Al_2O_3.

Note on XPS: O1s spectrum was fitted to four peaks. The peaks centered at 529.8, 531.2, and 532.2 eV are likely lattice oxygens. Since the reported binding energies for oxygen in the nickel-, palladium-, and aluminum oxides overlap, it is difficult to assign these peaks with much confidence. Our hypothesis is that these correspond to NiO and PdO for 529.8 eV[2-4], Ni_2O_3, and Al_2O_3 for 531.15 eV[2,4-9] and terminal hydroxides at 532.16 eV[9]. The fourth peak at 533.6 eV is characteristic of adsorbed water.[10]

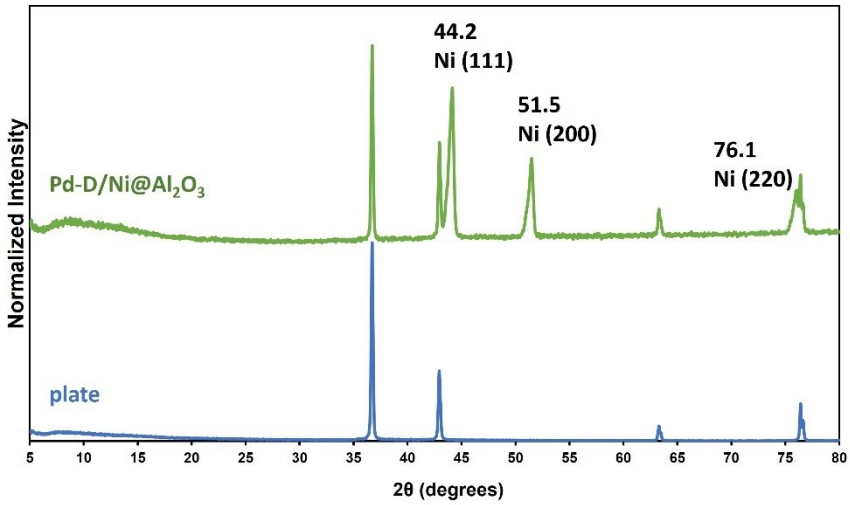

Fig. S10 Powder x-ray diffraction measurement of **Pd-D/Ni@Al_2O_3**.

Catalysis experiments:

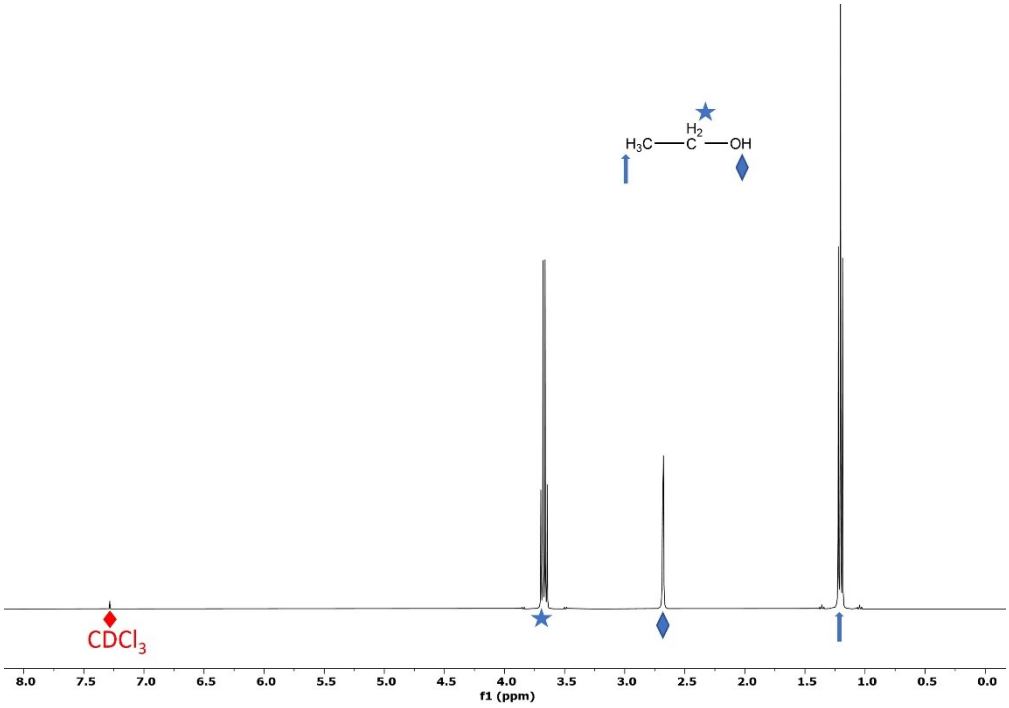

Fig. S11 ^{1}H NMR spectrum (400 MHz) of ethanol that was used as a solvent in all the catalytic systems.

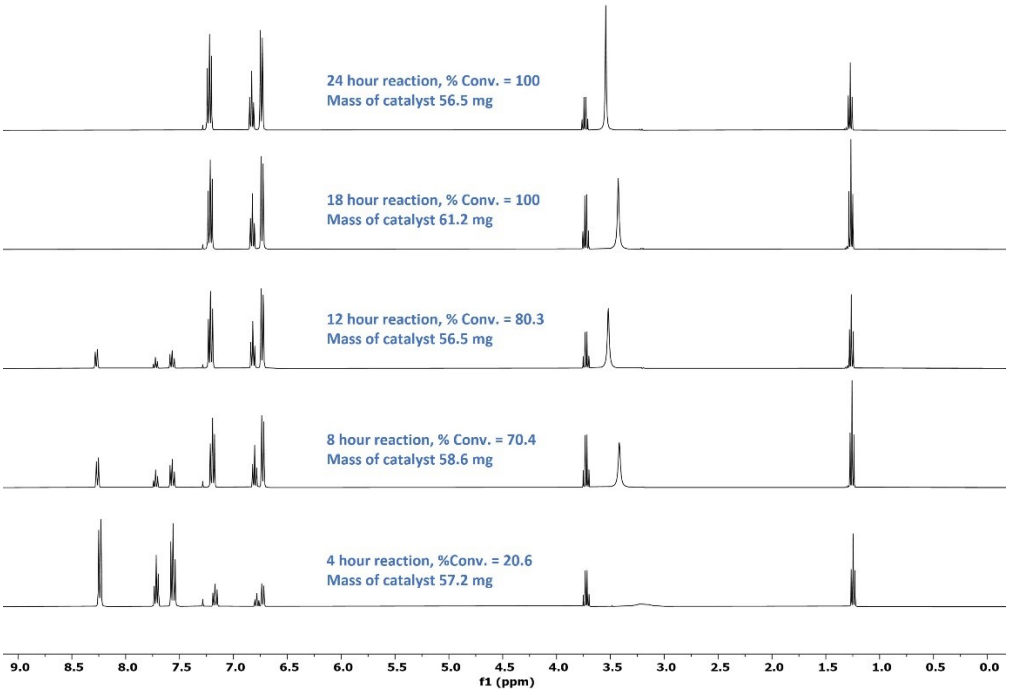

Fig. S12 ^{1}H NMR spectrum (400 MHz) of nitrobenzene hydrogenation as a function of time. Each trial uses a different piece of catalyst of similar weight. Reaction parameters: 1 mmol nitrobenzene, 3 bar H_2 gas, at 50 °C.

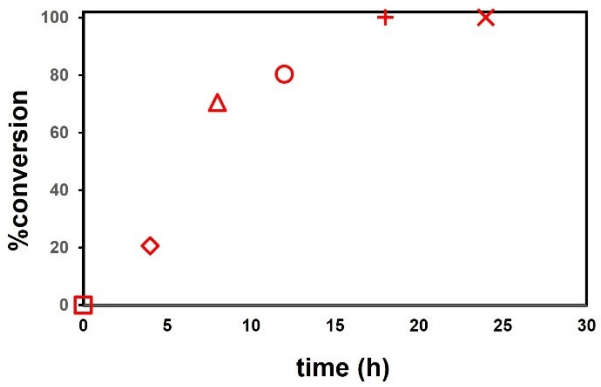

Fig. S13 % conversion of nitrobenzene to aniline as a function of time (see Fig. S12) under the following parameters: 1 mmol nitrobenzene, 3 bar H_2 gas, at 50 °C. Each marker is different to highlight that every trial is conducted by a different piece of catalyst of similar weight.

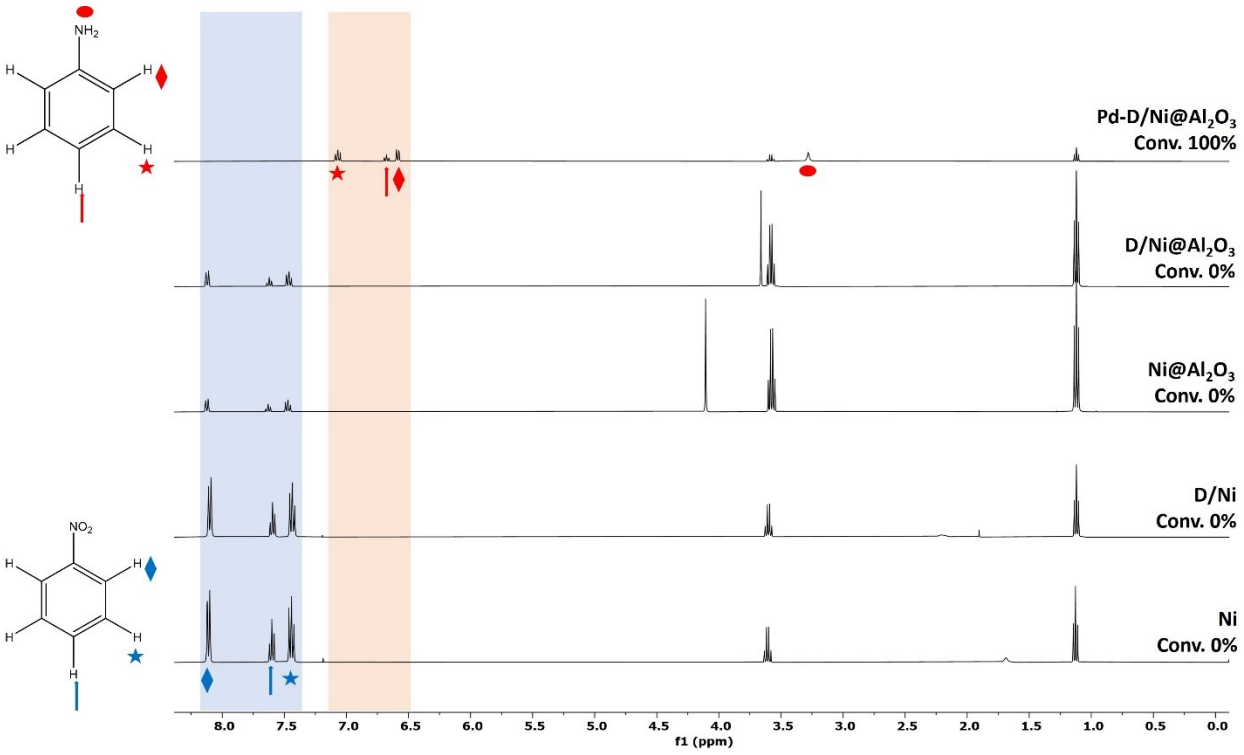

Fig. S14 ^{1}H NMR spectrum (400 MHz, $CDCl_3$) of isolated products after 18 hours for the reaction of 1 mmol nitrobenzene, 5 mL ethanol, and 3 bar H_2 gas over 61.2 mg Pd-D/Ni@Al_2O_3, 59 mg D/Ni@Al_2O_3, 65.4 mg Ni@Al_2O_3, 61.7 mg D/Ni, and 59.8 mg Ni materials, respectively. *Note 0% conversion in the absence of Pd.*

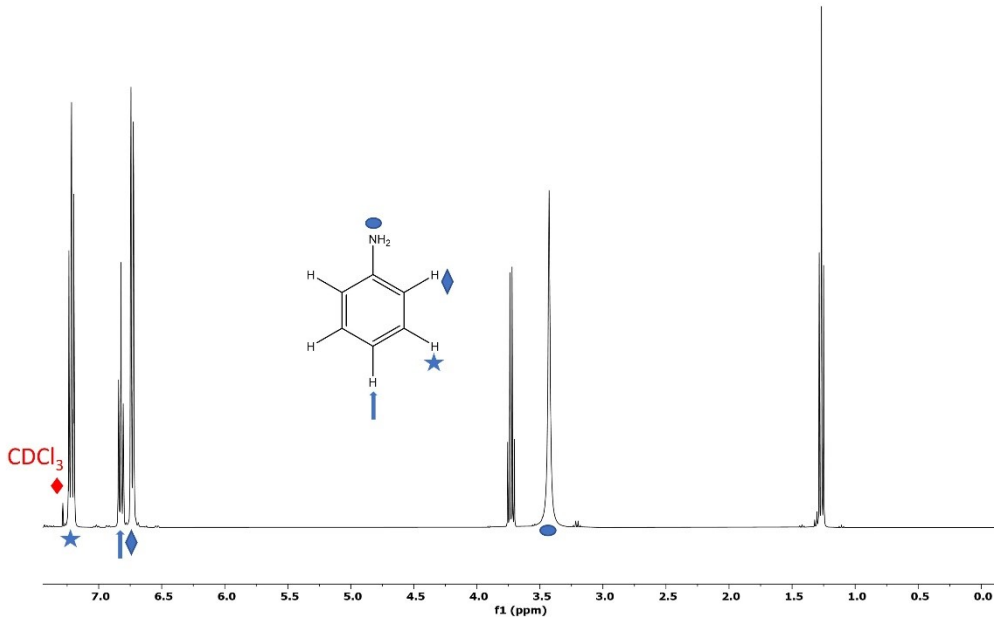

Fig. S15 ^{1}H NMR spectrum (400 MHz, $CDCl_3$) of isolated products of reaction **a**, Scheme 1. **Pd-D/Ni@Al_2O_3** = 61.2 mg.

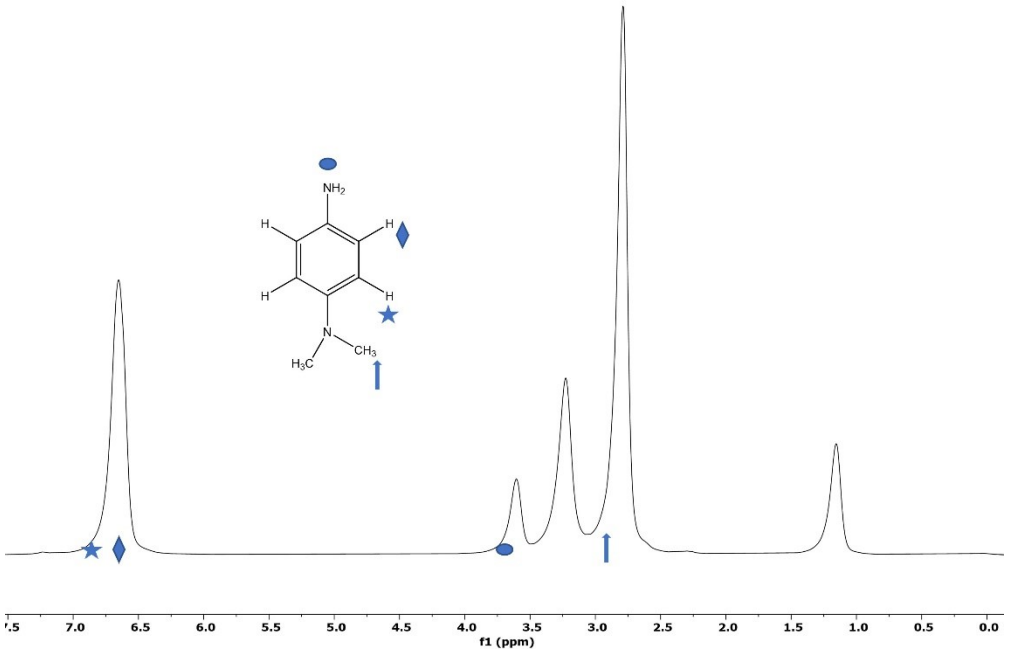

Fig. S16 ^{1}H NMR spectrum (400 MHz, $CDCl_3$) of isolated products of reaction **b**, Scheme 1. **Pd-D/Ni@Al_2O_3** = 60.0 mg.

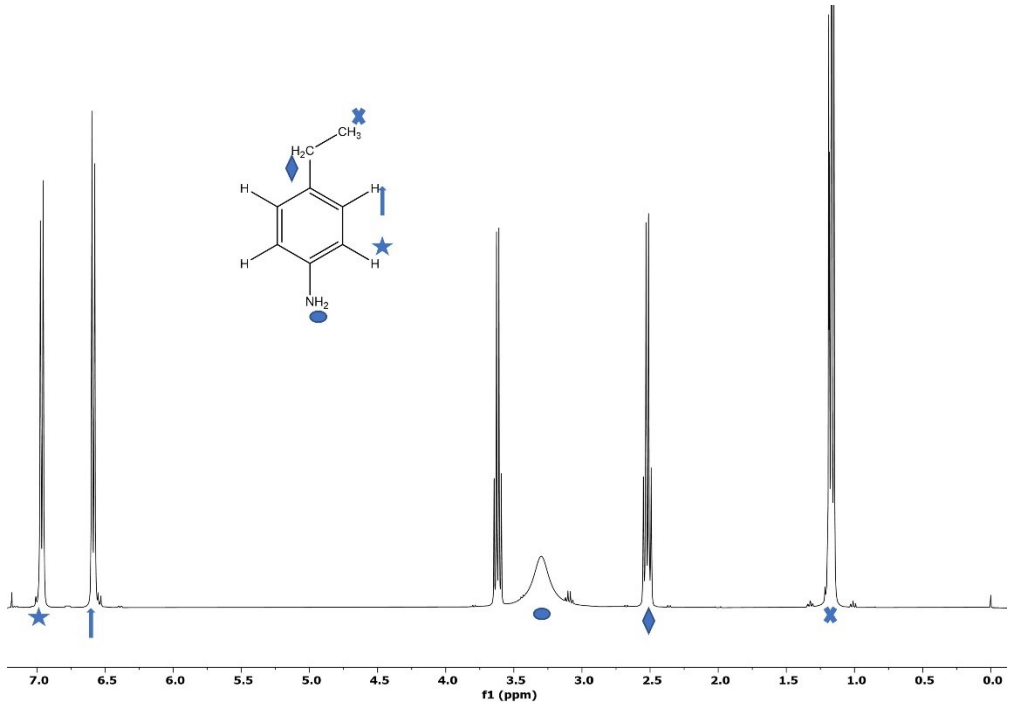

Fig. S17 ^{1}H NMR spectrum (400 MHz, $CDCl_3$) of isolated products of reaction **c**, Scheme 1. **Pd-D/Ni@Al_2O_3** = 59.7 mg.

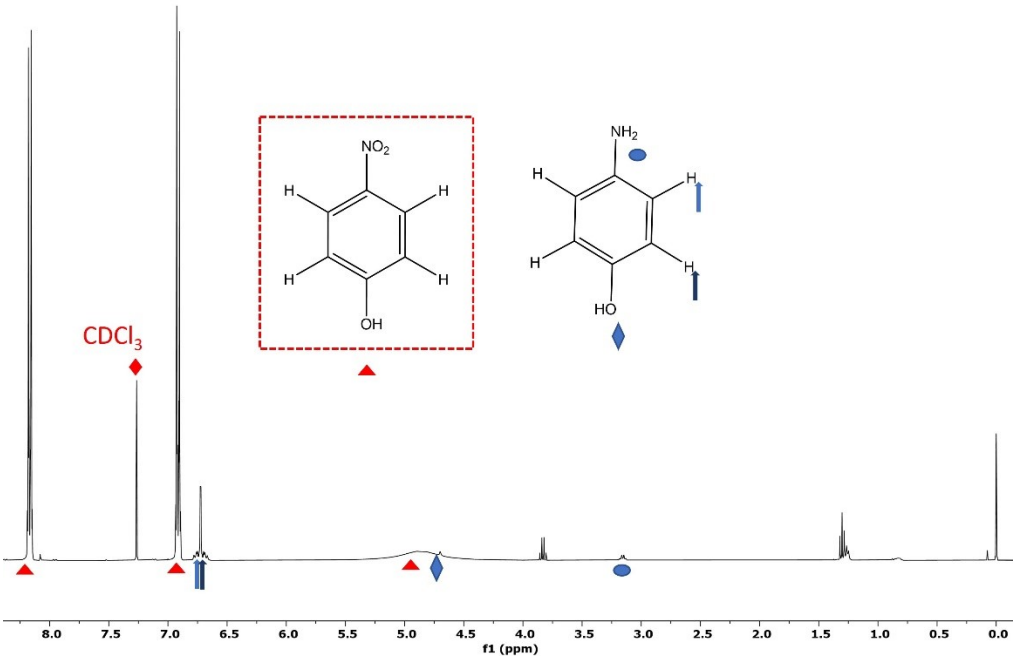

Fig. S18 ^{1}H NMR spectrum (400 MHz, $CDCl_3$) of isolated products of reaction **d**, Scheme 1. **Pd-D/Ni@Al_2O_3** = 59.8 mg.

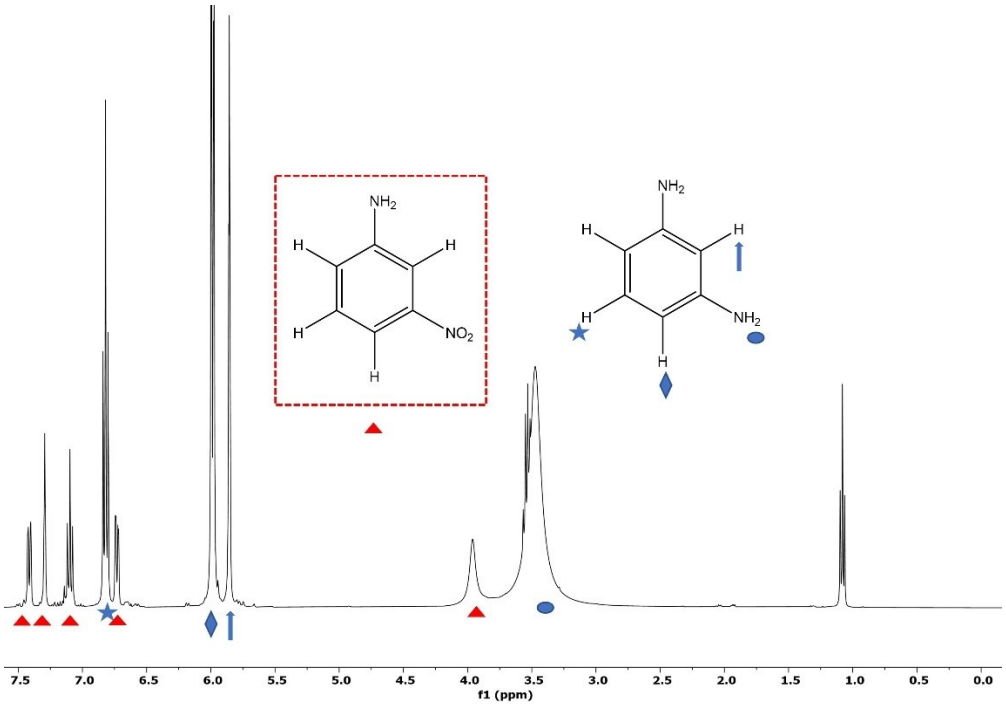

Fig. S19 ^{1}H NMR spectrum (400 MHz, $CDCl_3$) of isolated products of reaction **e**, Scheme 1. **Pd-D/Ni@Al_2O_3** = 59.5 mg.

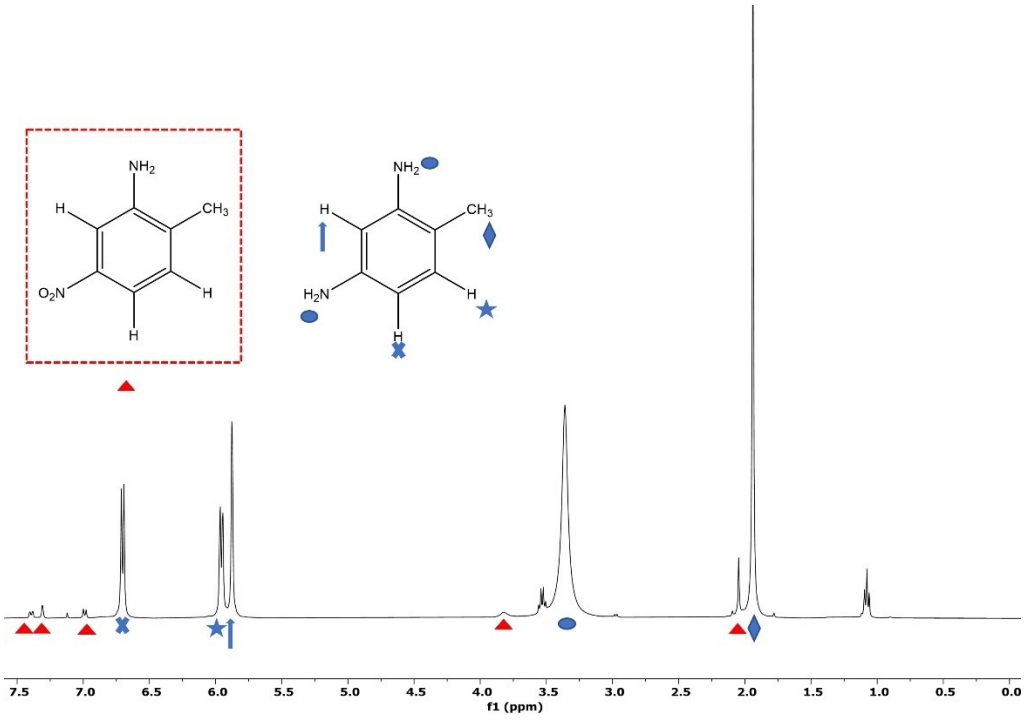

Fig. S20 ^{1}H NMR spectrum (400 MHz, $CDCl_3$) of isolated products of reaction **f**, Scheme 1. **Pd-D/Ni@Al_2O_3** = 58.5 mg.

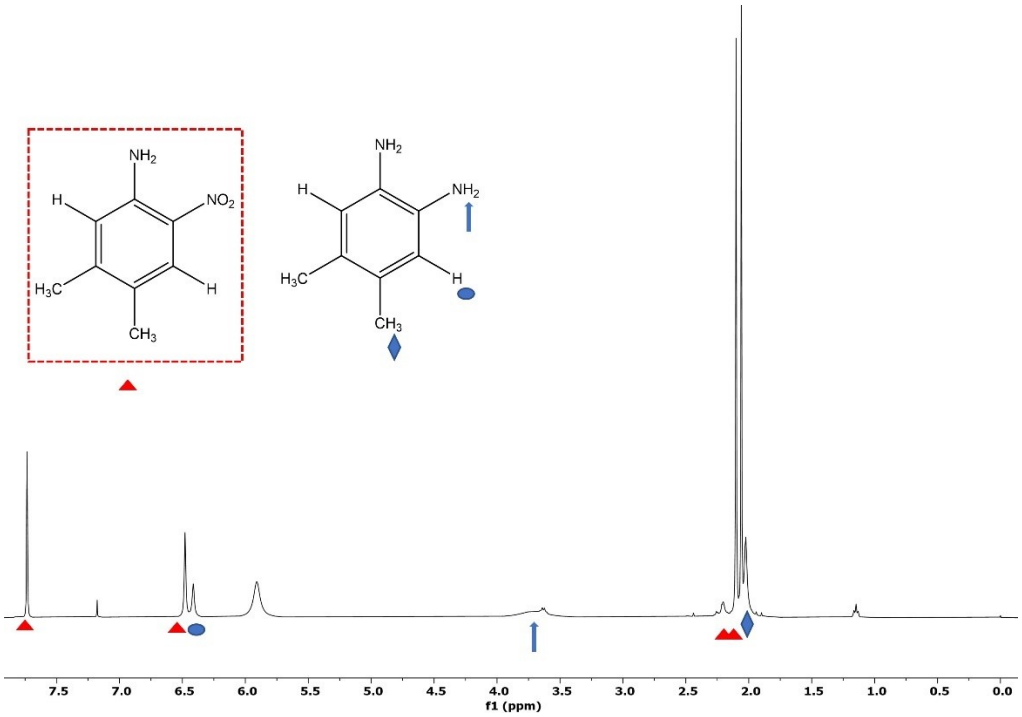

Fig. S21 ^{1}H NMR spectrum (400 MHz, $CDCl_3$) of isolated products of reaction **g**, Scheme 1. **Pd-D/Ni@Al_2O_3** = 61.6 mg.

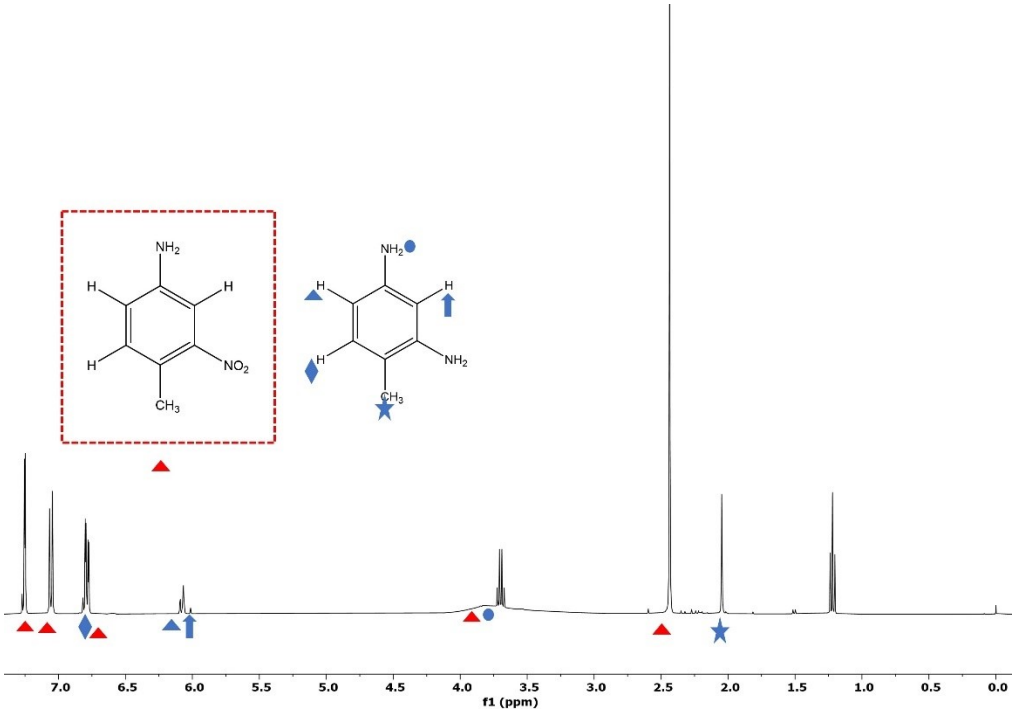

Fig. S22 ^{1}H NMR spectrum (400 MHz, $CDCl_3$) of isolated products of reaction **h**, Scheme 1. **Pd-D/Ni@Al_2O_3** = 60.7 mg.

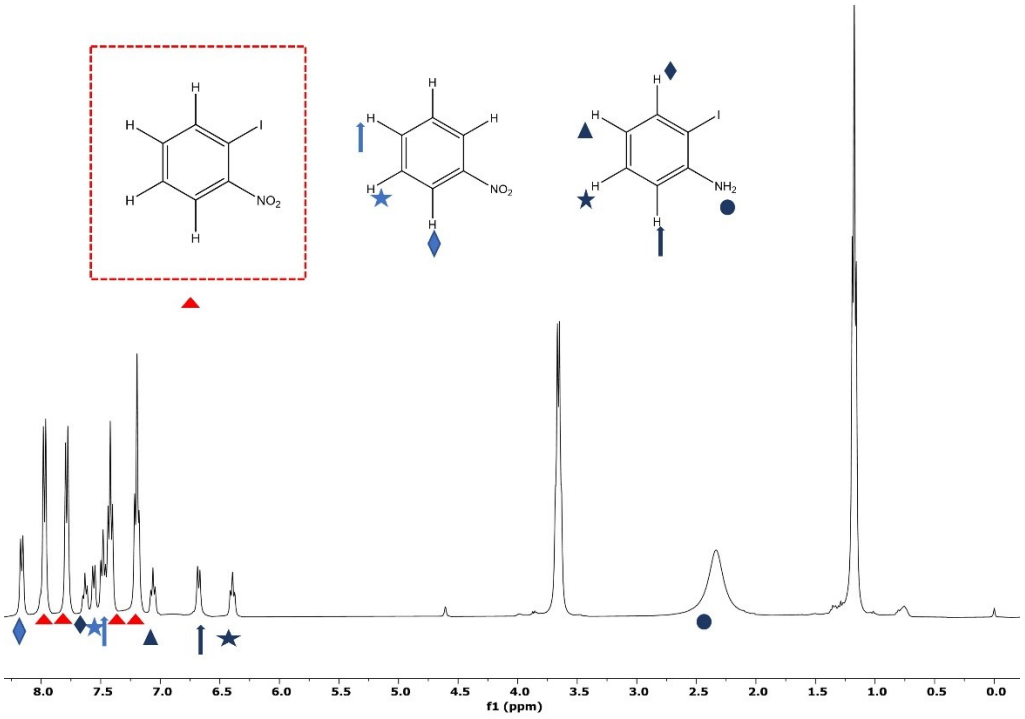

Fig. S23 ^{1}H NMR spectrum (400 MHz, $CDCl_3$) of isolated products of reaction **i**, Scheme 1. **Pd-D/Ni@Al_2O_3** = 59.0 mg.

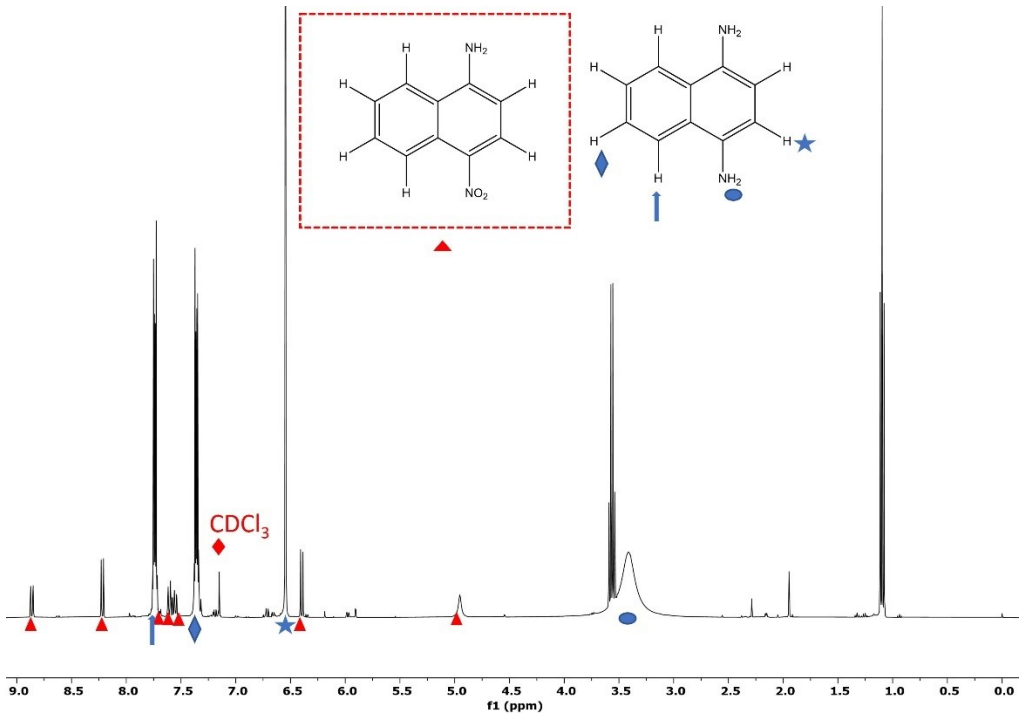

Fig. S24 ^{1}H NMR spectrum (400 MHz, $CDCl_3$) of isolated products of reaction **j**, Scheme 1. **Pd-D/Ni@Al_2O_3** = 61.5 mg.

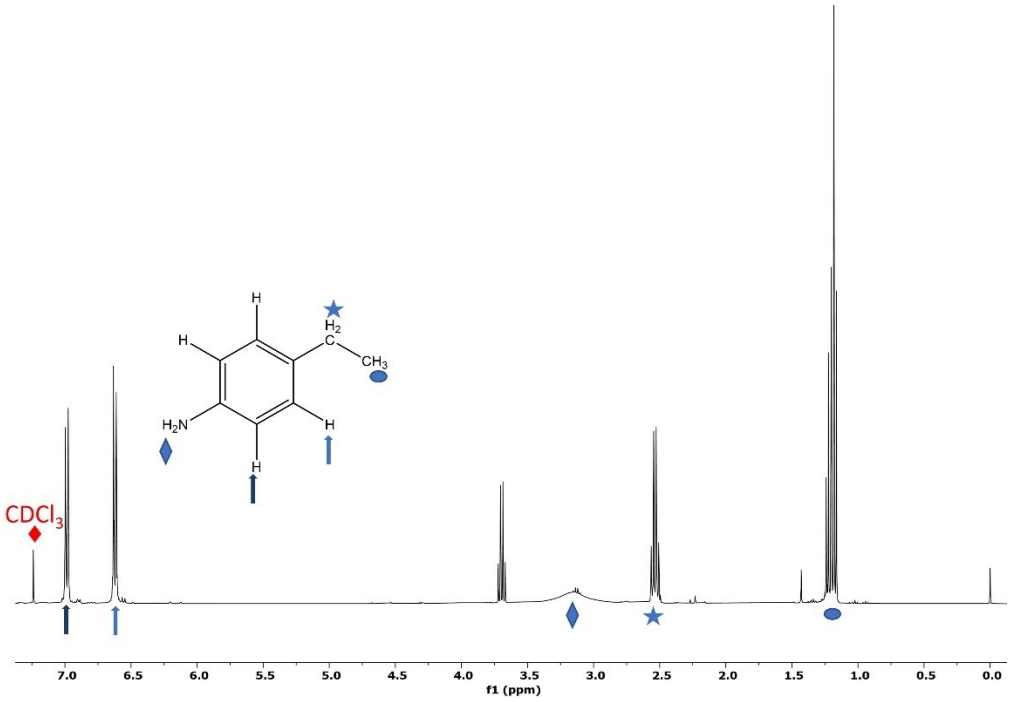

Fig. S25 ^{1}H NMR spectrum (400 MHz, $CDCl_3$) of isolated products of reaction **k**, Scheme 1. **Pd-D/Ni@Al_2O_3** = 58.5 mg.

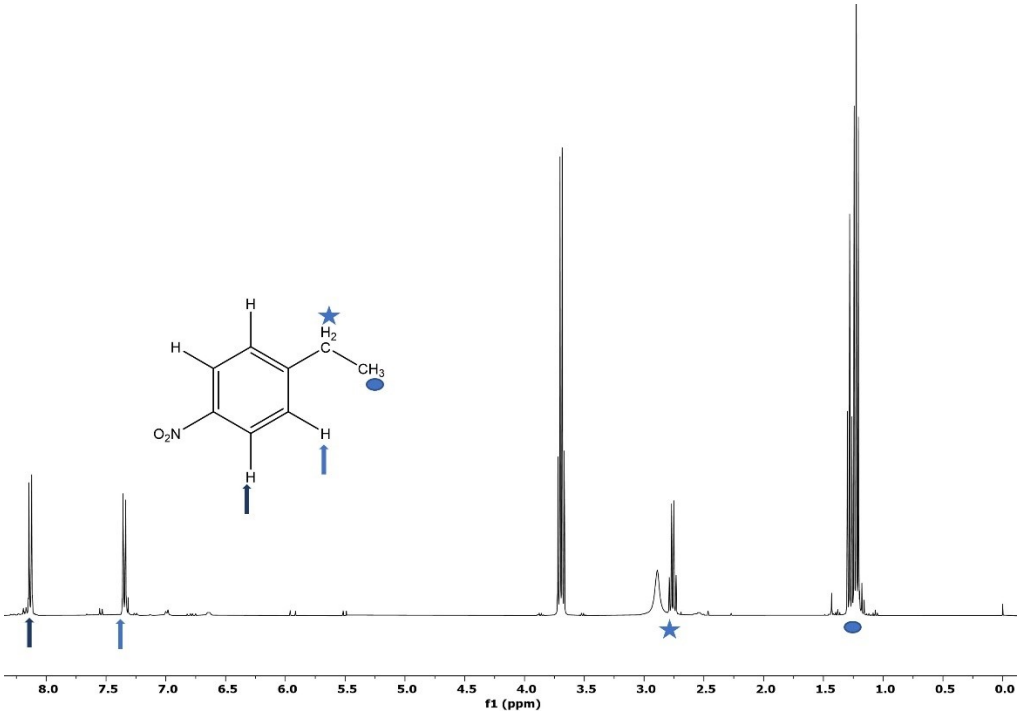

Fig. S26 ^{1}H NMR spectrum (400 MHz, $CDCl_3$) of isolated products of reaction **l**, Scheme 1. **Pd-D/Ni@Al_2O_3** = 59.0 mg.

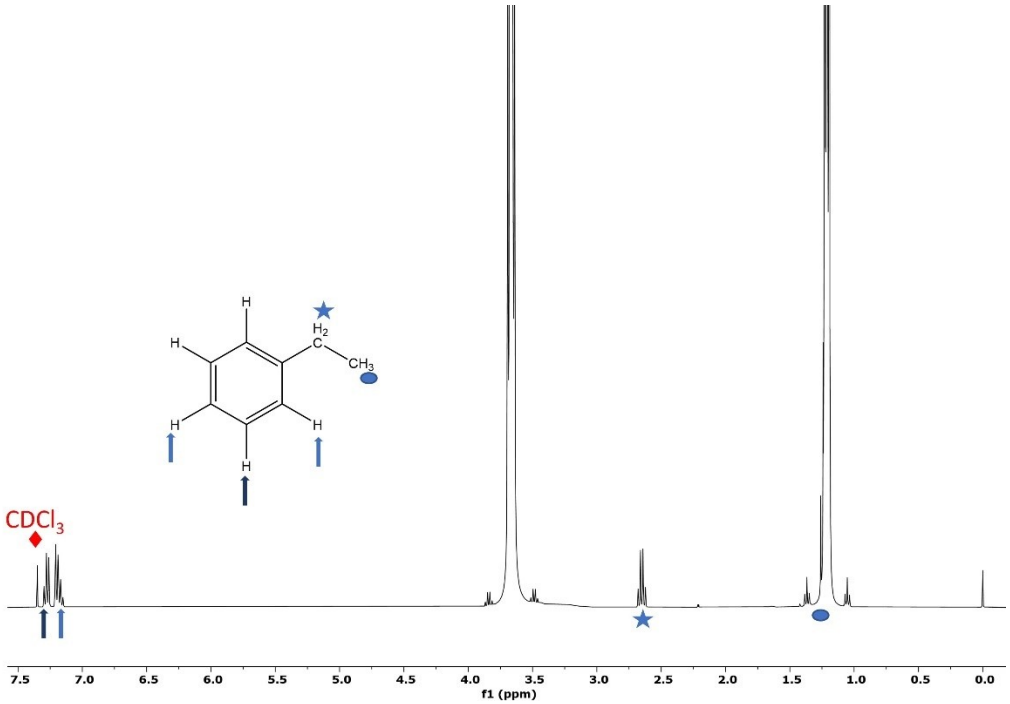

Fig. S27 ^{1}H NMR spectrum (400 MHz, $CDCl_3$) of isolated products of reaction **m**, Scheme 1. **Pd-D/Ni@Al_2O_3** = 59.7 mg.

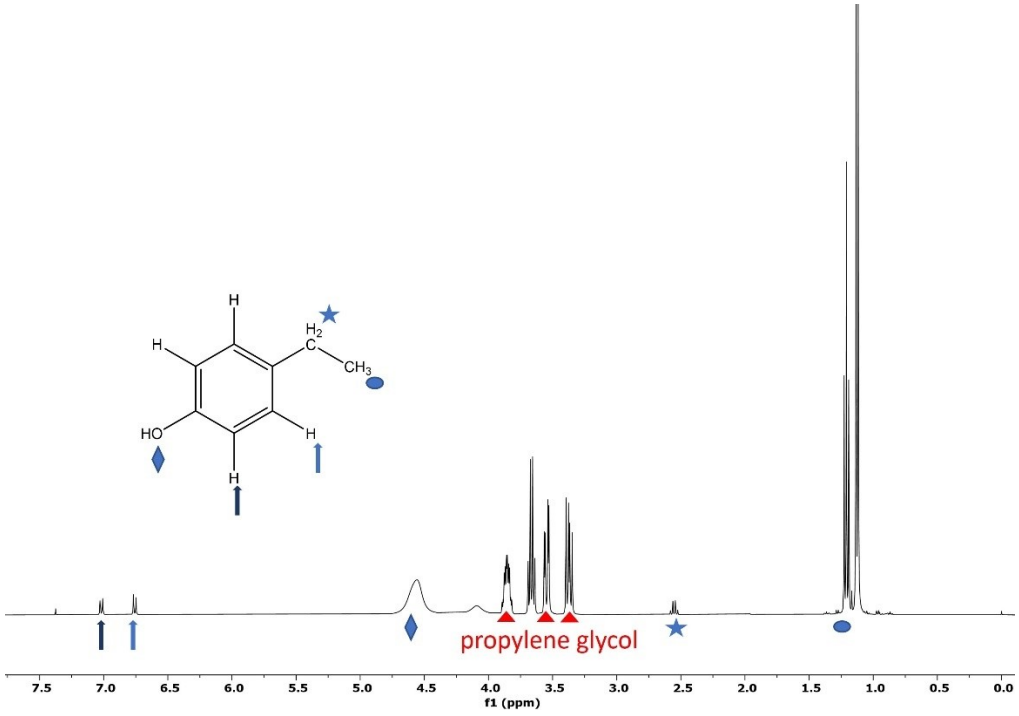

Fig. S28 ^{1}H NMR spectrum (400 MHz, $CDCl_3$) of isolated products of reaction **n**, Scheme 1. **Pd-D/Ni@Al_2O_3** = 60.2 mg. *Reaction is not impeded by the presence of propylene glycol stabilizer.*

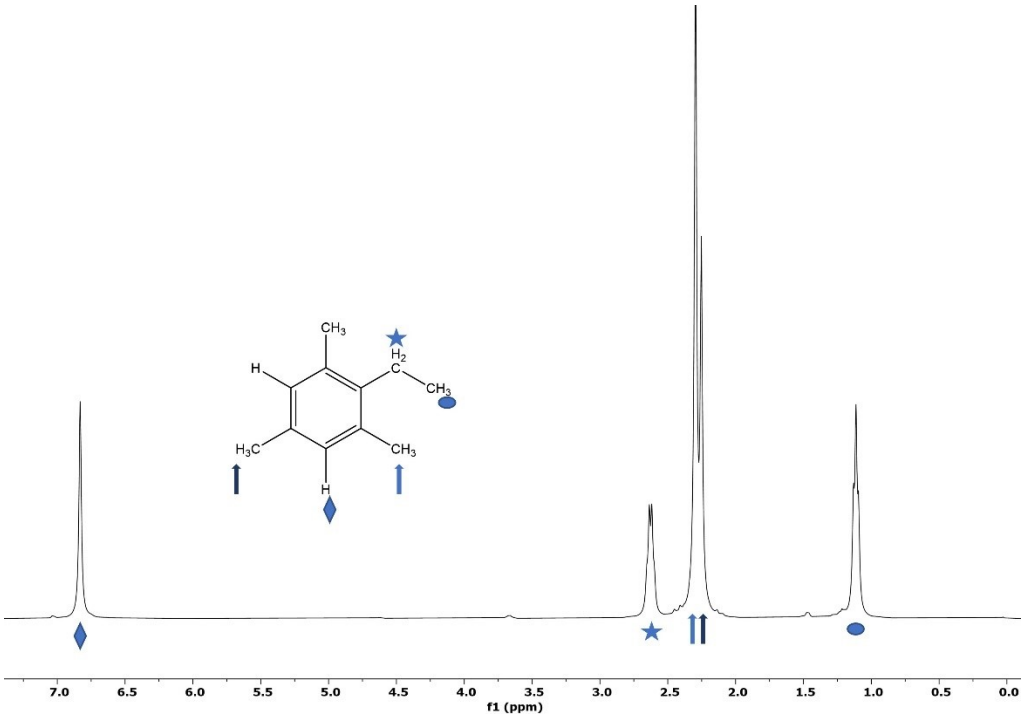

Fig. S29 ^{1}H NMR spectrum (400 MHz, $CDCl_3$) of isolated products of reaction **o**, Scheme 1. **Pd-D/Ni@Al_2O_3** = 62.0 mg.

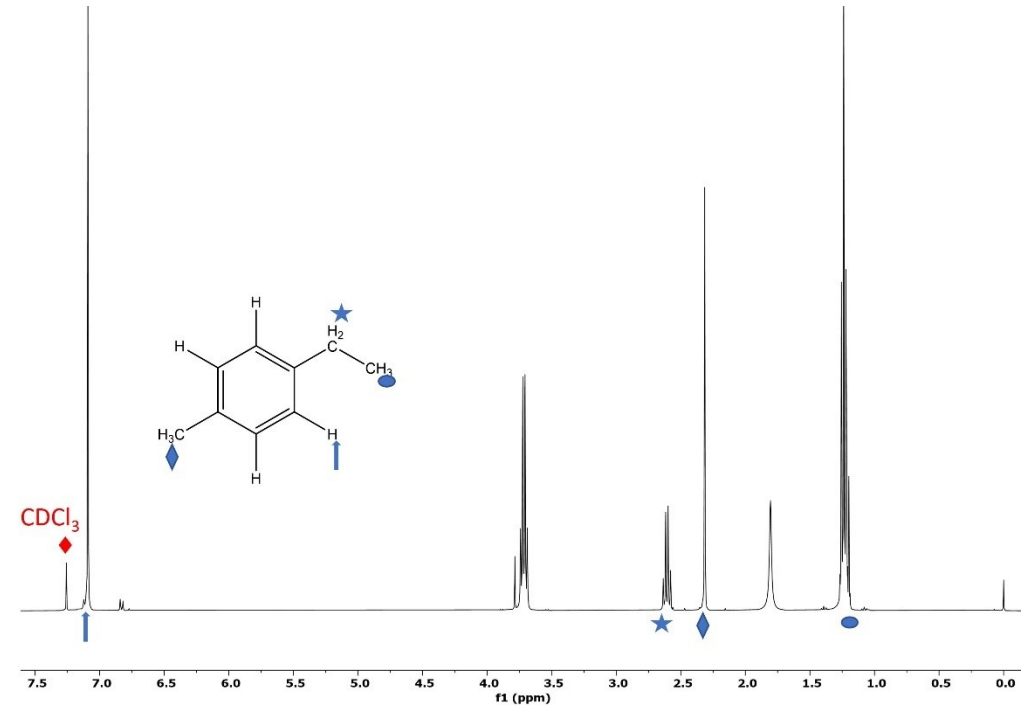

Fig. S30 ^{1}H NMR spectrum (400 MHz, $CDCl_3$) of isolated products of reaction **p**, Scheme 1. **Pd-D/Ni@Al_2O_3** = 56.8 mg.

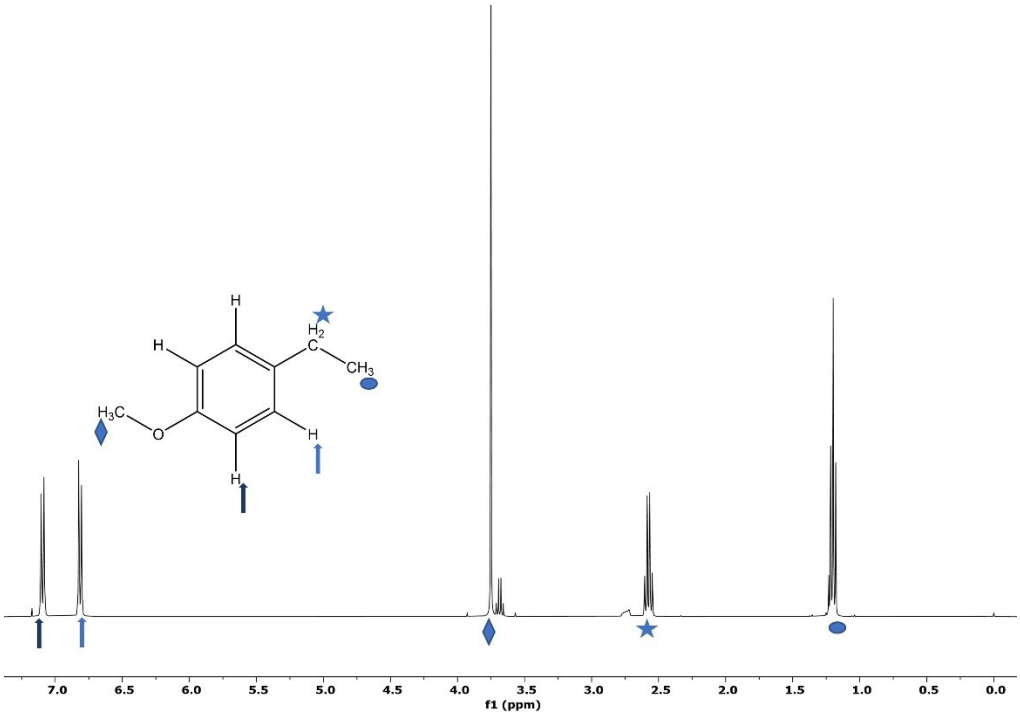

Fig. S31 ^{1}H NMR spectrum (400 MHz, $CDCl_3$) of isolated products of reaction **q**, Scheme 1. **Pd-D/Ni@Al_2O_3** = 58.0 mg.

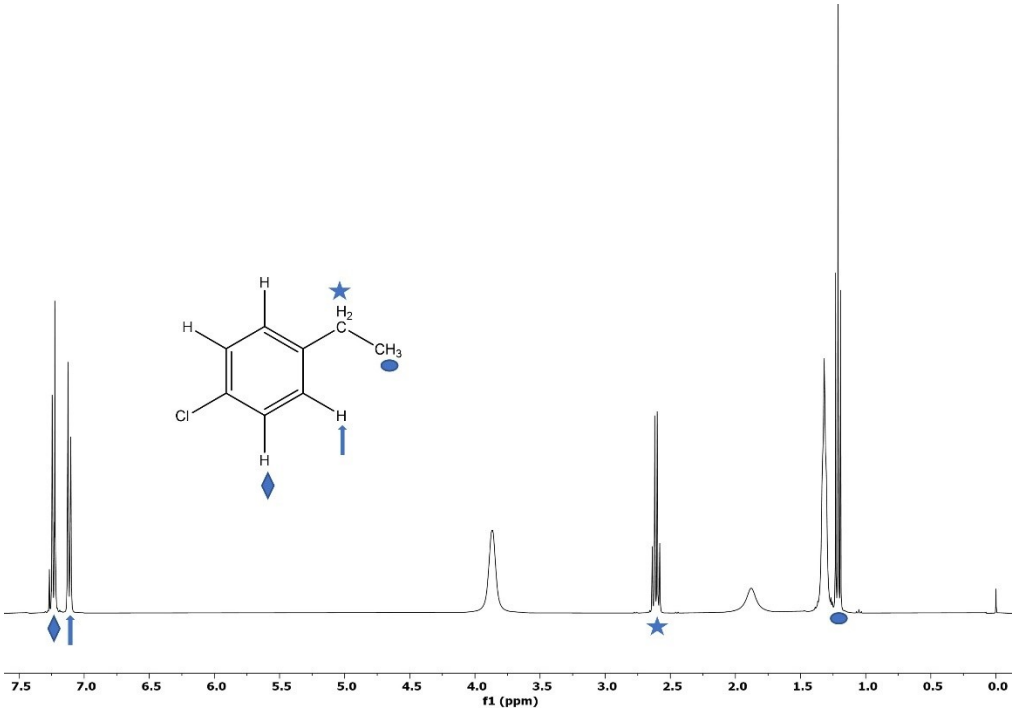

Fig. S32 ^{1}H NMR spectrum (400 MHz, $CDCl_3$) of isolated products of reaction **r**, Scheme 1. **Pd-D/Ni@Al_2O_3** = 61.8 mg.

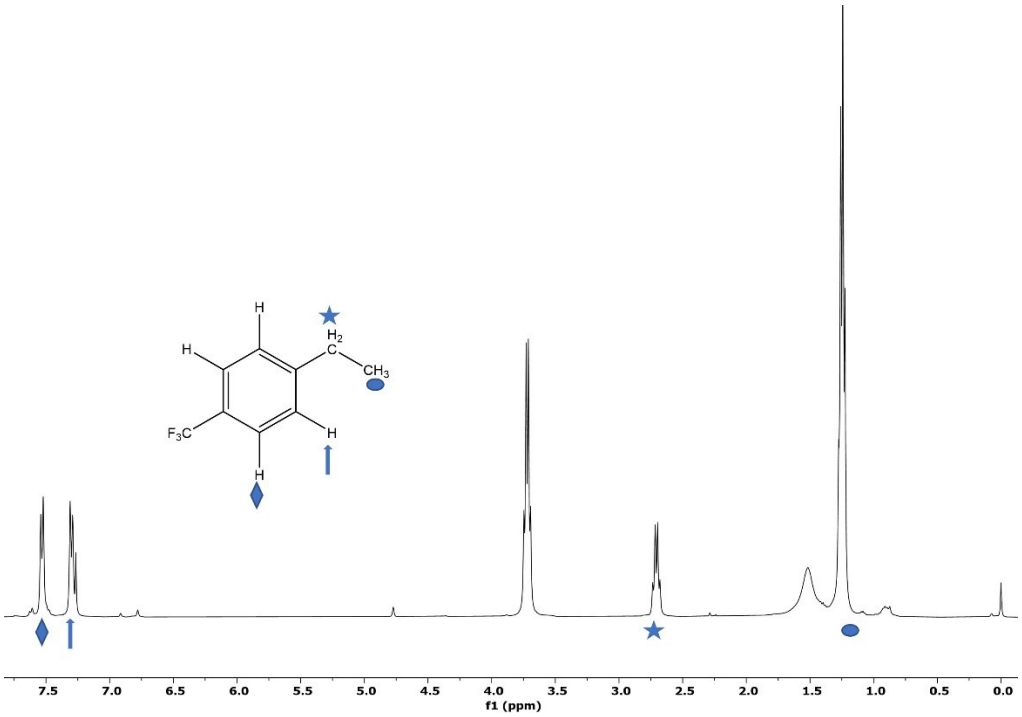

Fig. S33 ^{1}H NMR spectrum (400 MHz, $CDCl_3$) of isolated products of reaction **s**, Scheme 1. **Pd-D/Ni@Al_2O_3** = 62.0 mg.

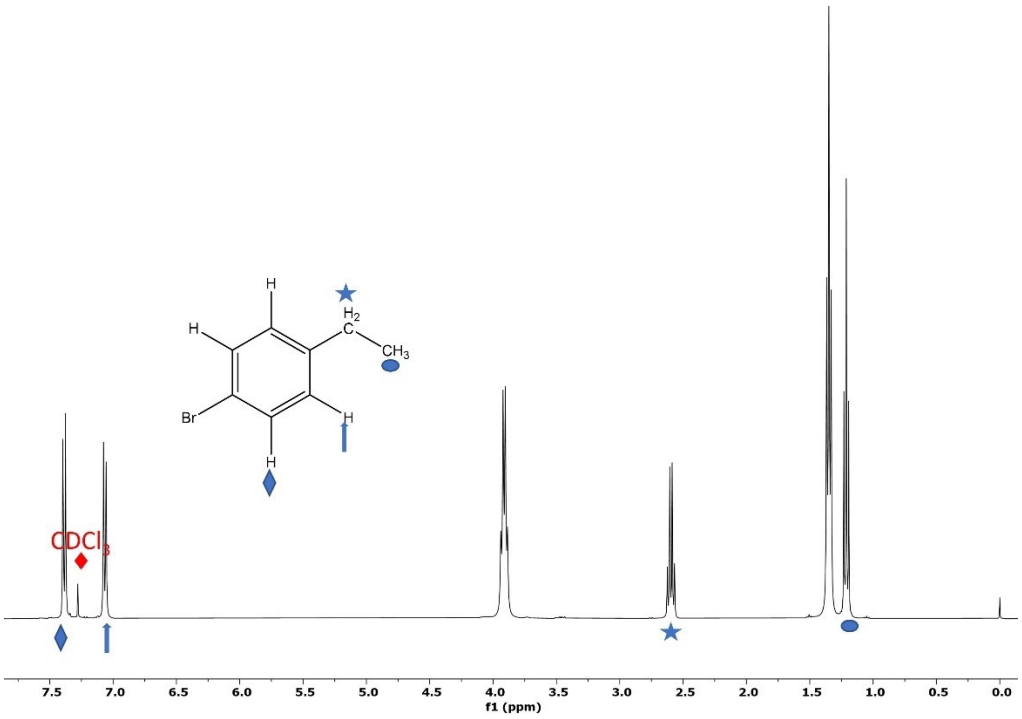

Fig. S34 ^{1}H NMR spectrum (400 MHz, $CDCl_3$) of isolated products of reaction **t**, Scheme 1. **Pd-D/Ni@Al_2O_3** = 57.4 mg.

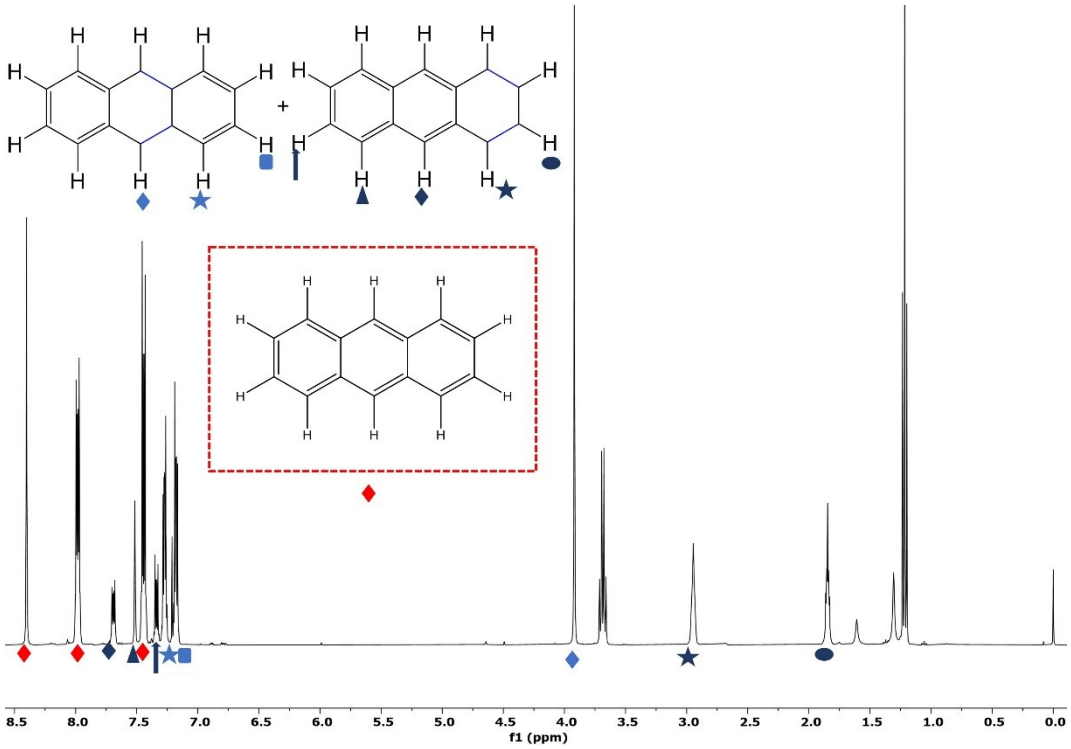

Fig. S35 ^{1}H NMR spectrum (400 MHz, $CDCl_3$) of isolated products of reaction **u** (1 mmol Anthracene, 3 bar H_2 gas, *at 50 °C*), Scheme 1. **Pd-D/Ni@Al_2O_3** = 60.0 mg.

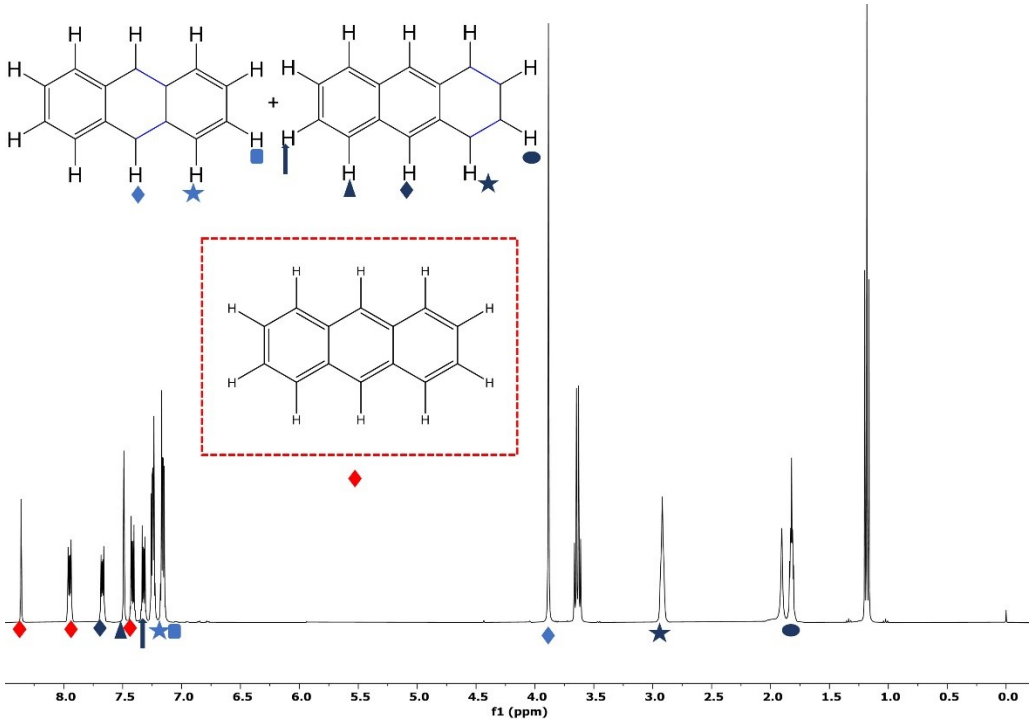

Fig. S36 ^{1}H NMR spectrum (400 MHz, $CDCl_3$) of isolated products of reaction **u** (0.5 mmol Anthracene, 3 bar H_2 gas, *at 100 °C*), Scheme 1. **Pd-D/Ni@Al_2O_3** = 59.9 mg.

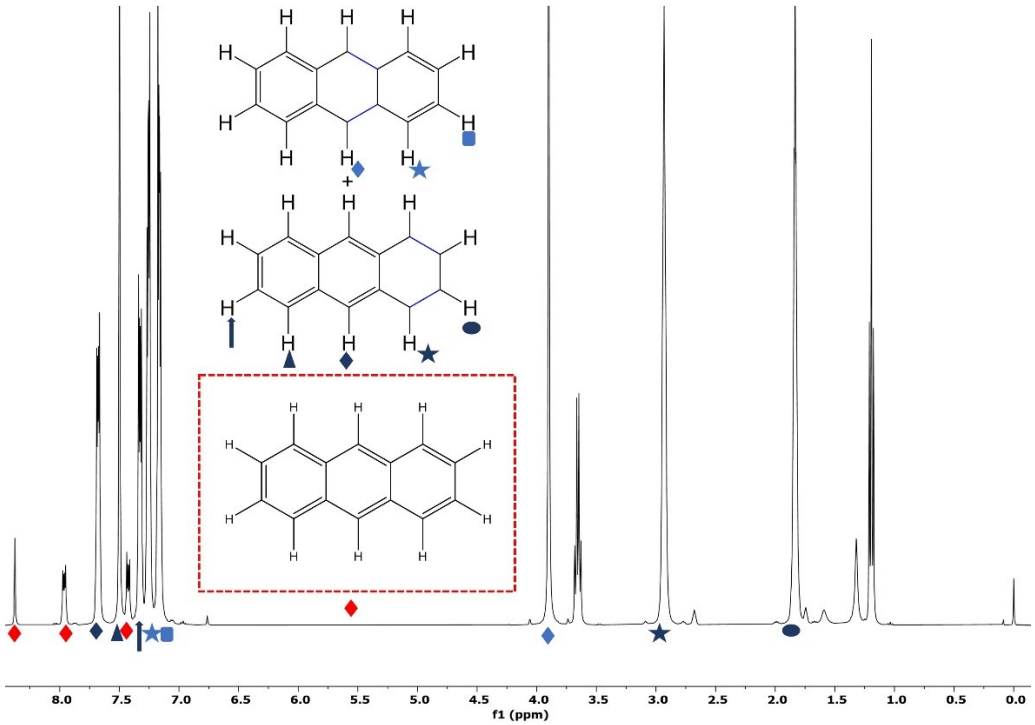

Fig. S37 ^{1}H NMR spectrum (400 MHz, $CDCl_3$) of isolated products of reaction **u** (0.5 mmol Anthracene, 5 bar H_2 gas, *at 100 °C*), Scheme 1. **Pd-D/Ni@Al_2O_3** = 60.8 mg.

Continuous Flow Catalysis Reactions

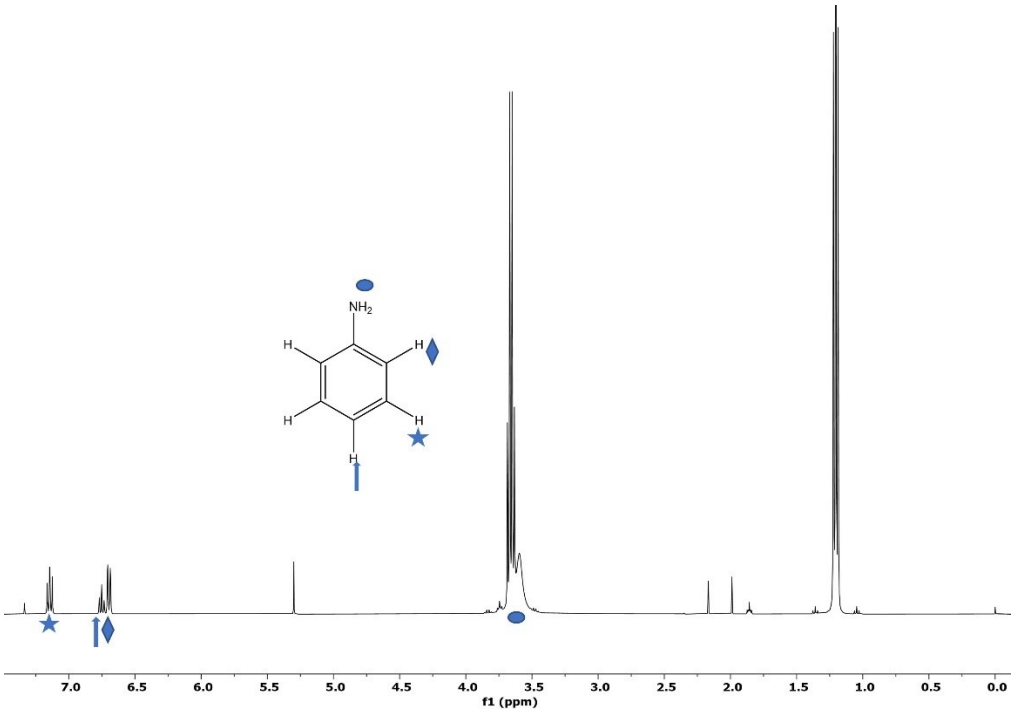

Fig. S38 ^{1}H NMR spectrum (400 MHz, $CDCl_3$) of isolated products of nitrobenzene hydrogenation. Parameter set Table 1,#1.

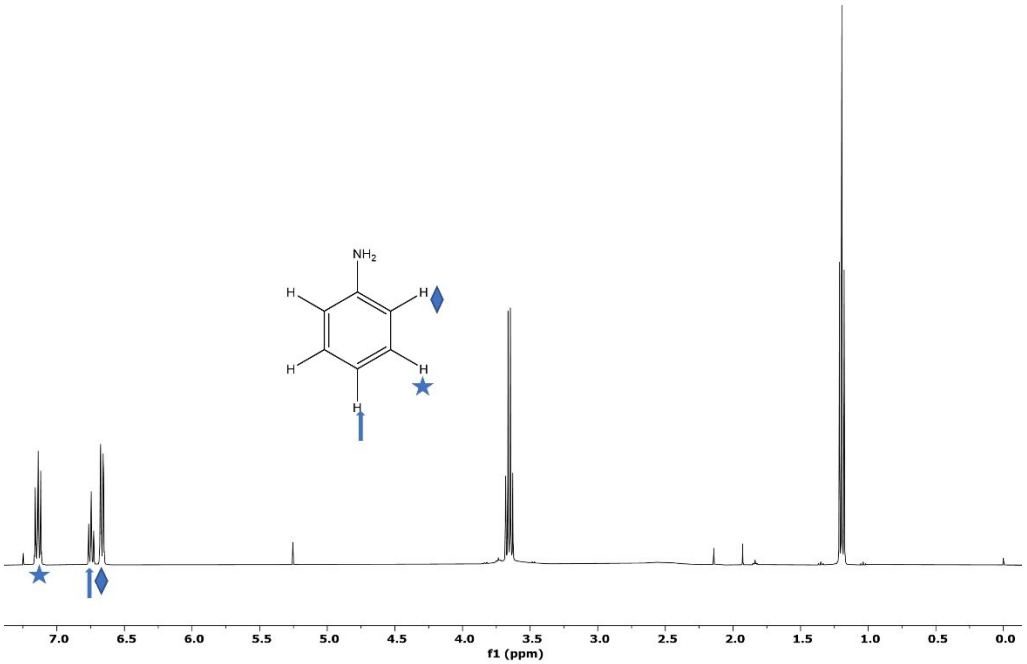

Fig. S39 ^{1}H NMR spectrum (400 MHz, $CDCl_3$) of isolated products of nitrobenzene hydrogenation. Parameter set Table 1,#2.

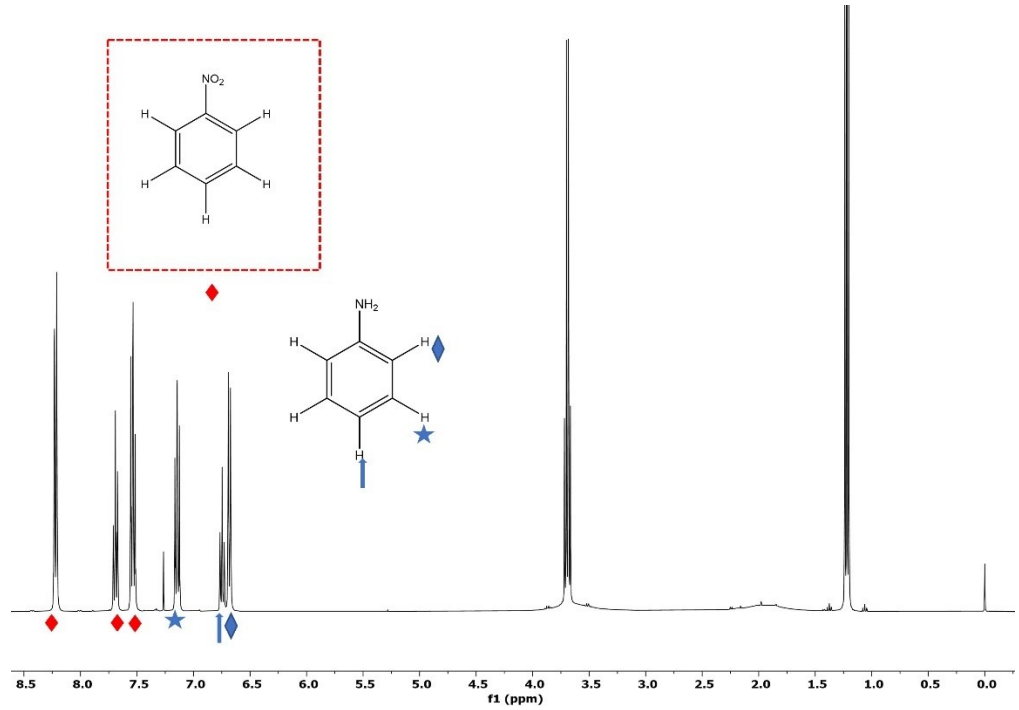

Fig. S40 ^{1}H NMR spectrum (400 MHz, $CDCl_3$) of isolated products of nitrobenzene hydrogenation. Parameter set Table 1,#3.

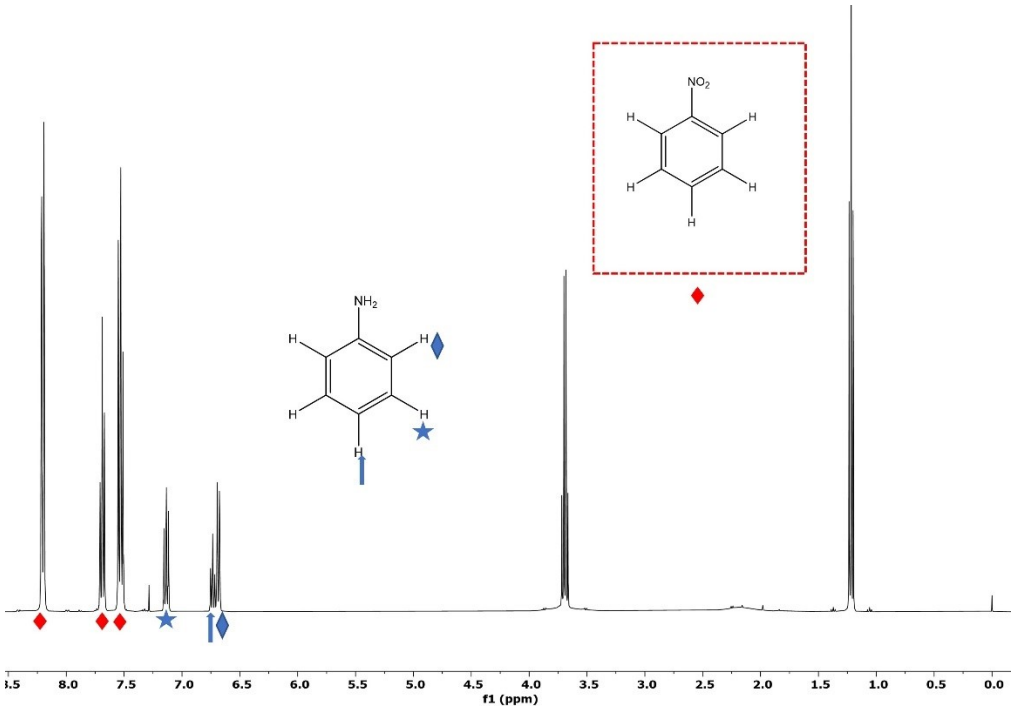

Fig. S41 ^{1}H NMR spectrum (400 MHz, $CDCl_3$) of isolated products of nitrobenzene hydrogenation. Parameter set Table 1,#4.

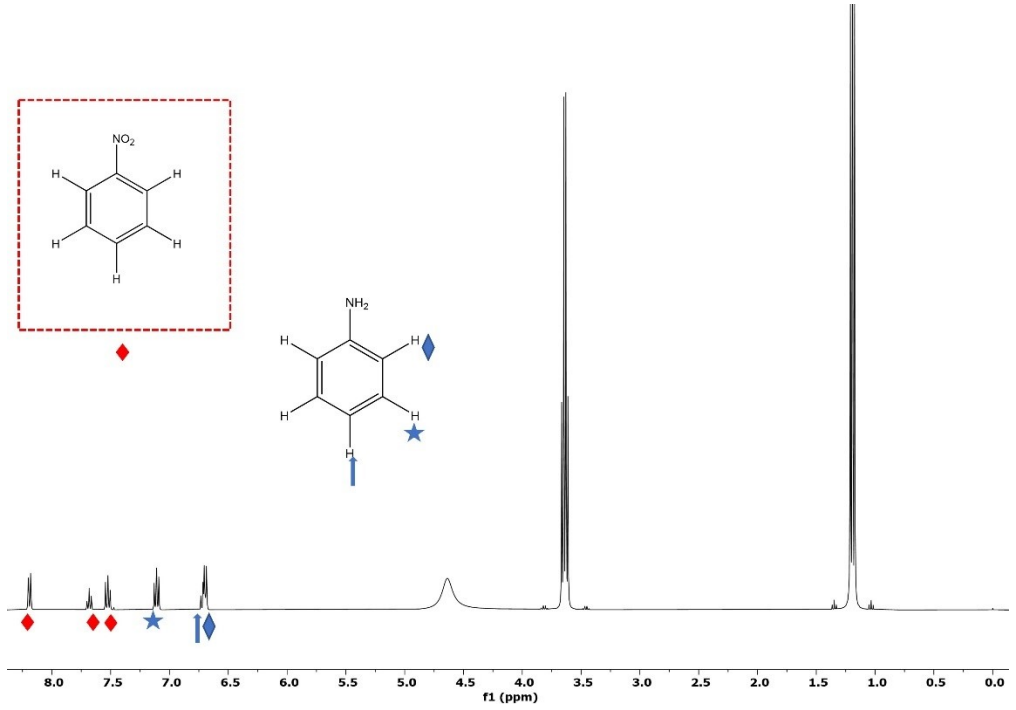

Fig. S42 ^{1}H NMR spectrum (400 MHz, $CDCl_3$) of isolated products of nitrobenzene hydrogenation. Parameter set Table 1,#5.

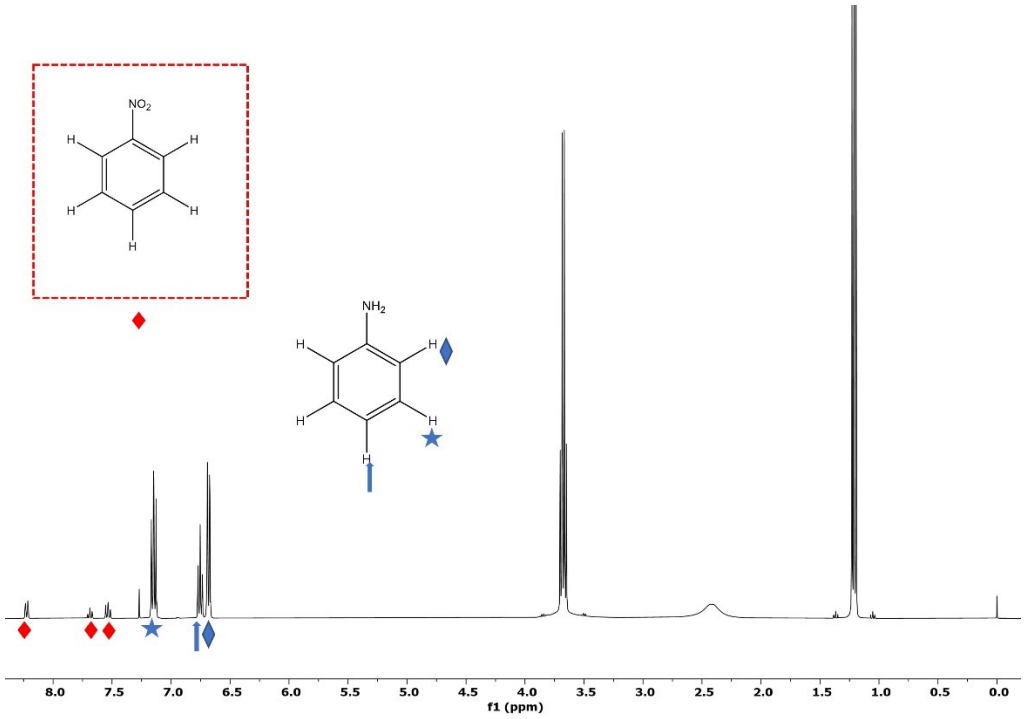

Fig. S43 ^{1}H NMR spectrum (400 MHz, $CDCl_3$) of isolated products of nitrobenzene hydrogenation. Parameter set Table 1,#6.

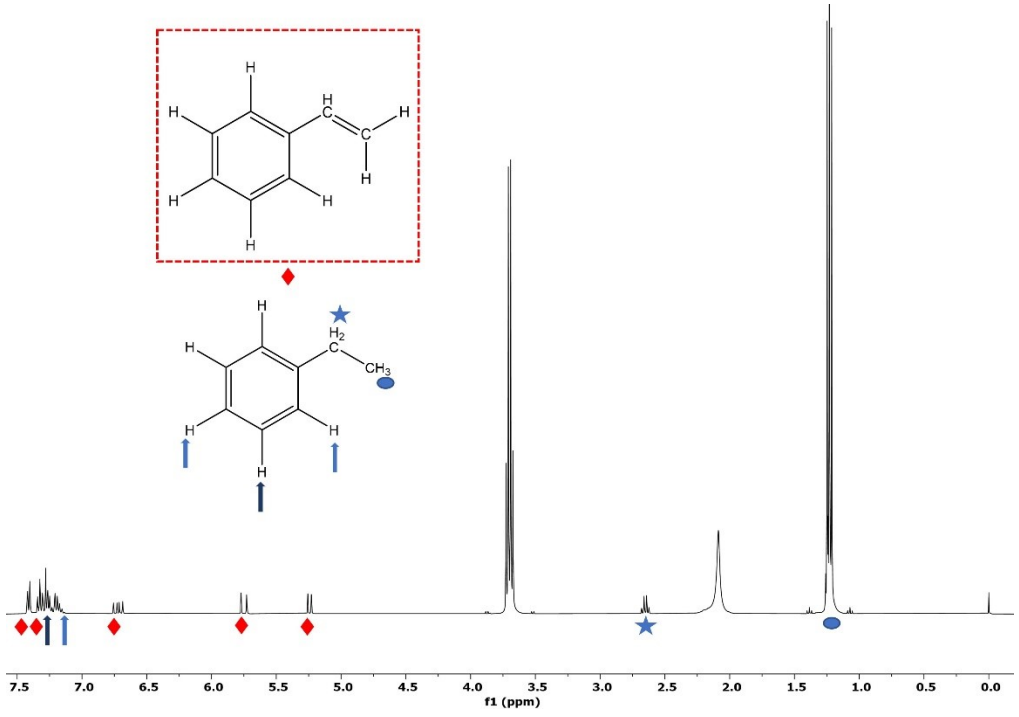

Fig. S44 ^{1}H NMR spectrum (400 MHz, $CDCl_3$) of isolated products of styrene hydrogenation. Parameter set Table 1,#7.

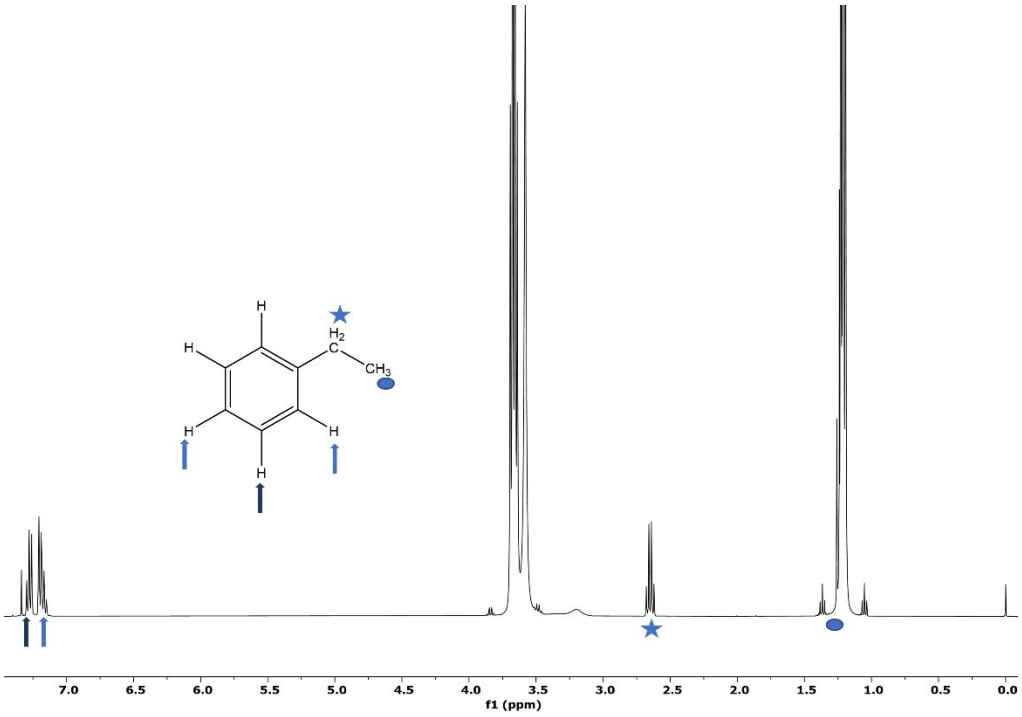

Fig. S45 ^{1}H NMR spectrum (400 MHz, $CDCl_3$) of isolated products of styrene hydrogenation. Parameter set Table 1,#8.

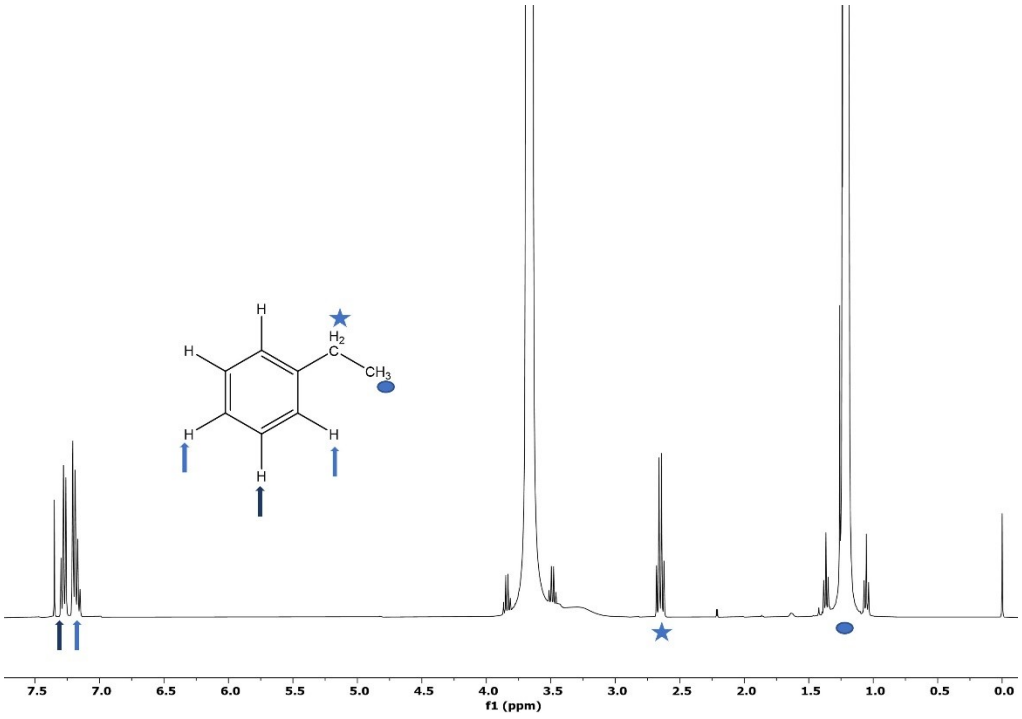

Fig. S46 ^{1}H NMR spectrum (400 MHz, $CDCl_3$) of isolated products of styrene hydrogenation. Parameter set Table 1,#9.

Recyclability Test

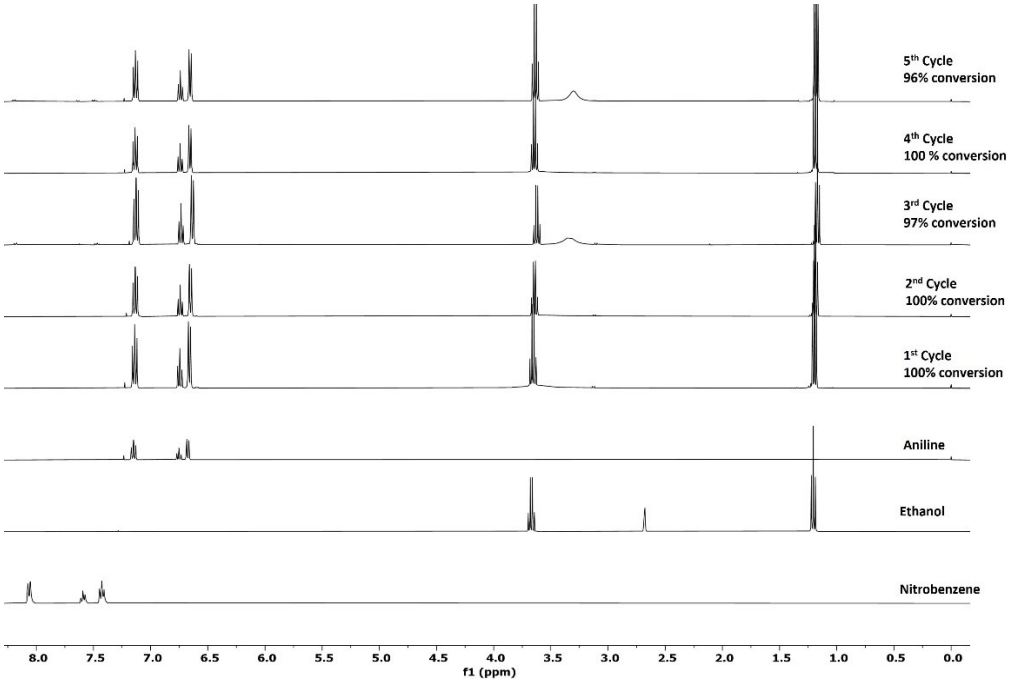

Fig. S47 ^{1}H NMR spectra (400 MHz, $CDCl_3$) for nitrobenzene hydrogenation recycling trials. Reaction parameters: 1 mmol nitrobenzene, 101.5 mg **Pd-D@NiAl$_2$O$_3$**, 4 bar H_2, T= 50 °C, t= 24 hours, 5 mL ethanol as a solvent.

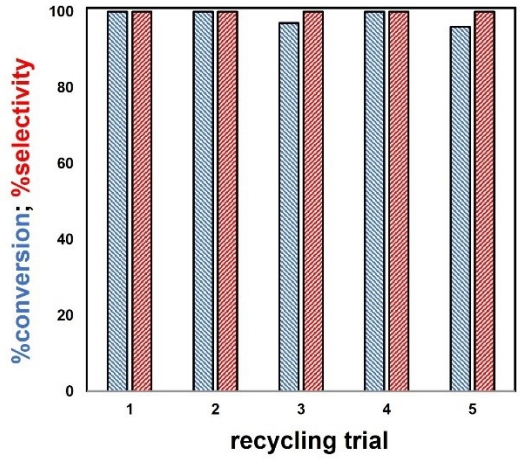

Fig. S48 % conversion and selectivity as a function of recycling trial. Reaction parameters: 1 mmol nitrobenzene, 101.5 mg **Pd-D@NiAl$_2$O$_3$**, 4 bar H_2, T= 50 °C, t= 24 hours, 5 mL ethanol as a solvent. *As the reaction only reaches completion at 18 h at 3 bar H_2, we extended the conditions slightly to approximate a more probable real-world reuse and recycle protocol.*

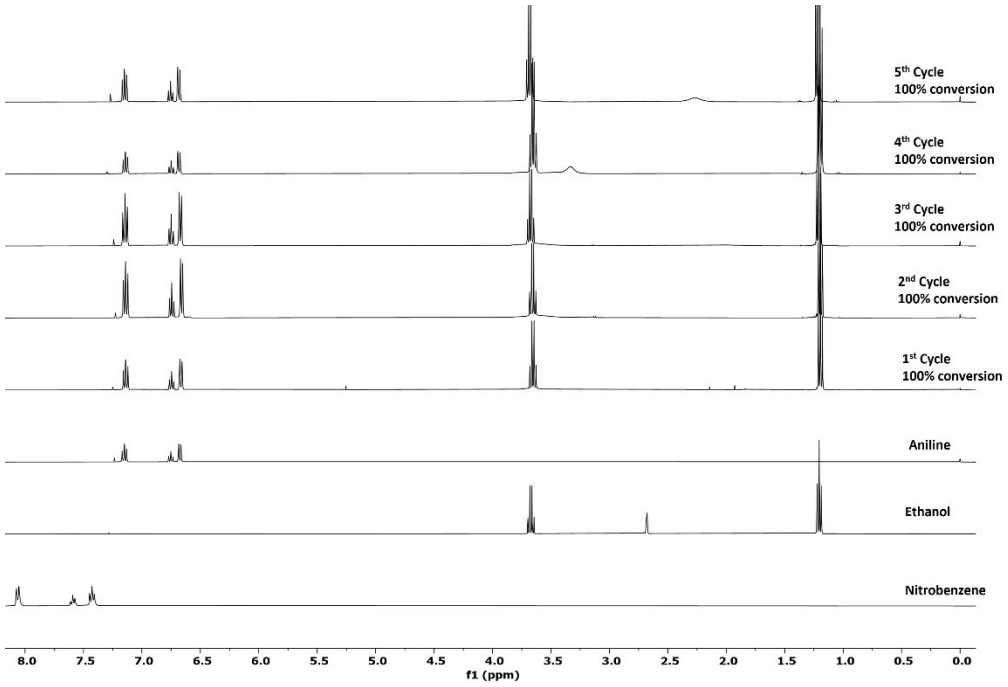

Fig. S49 ^{1}H NMR spectra (400 MHz, $CDCl_3$) for nitrobenzene hydrogenation recycling trials. Reaction parameters: 0.5 mmol nitrobenzene, 102.0 mg **Pd-D@NiAl$_2$O$_3$**, 4 bar H_2, T= 50 °C, t= 24 hours, 5 mL ethanol as a solvent. *We note that at lower nitrobenzene concentration we maintain complete conversion over 5 trials.*

Table S1 Comparison of catalytic activity with recent literature. *DIW = deionized water; all reactions performed in batch, TOF measured as a function of mol Pd. (*avg catalyst mass of 59.9 ± 1.5 mg)*

Catalyst	Substrate	solvent	Pd Mass %	t (h)	T (°C)	H_2 (bar)	TOF (h^{-1})	Conv. %	Ref.
Pd-D/Ni@Al_2O_3	nitrobenzene	ethanol	0.017	18	50	3	*573	99.9	*this work*
Pd-D/Ni@Al_2O_3	styrene	ethanol	0.017	18	50	3	*573	99.9	*this work*
Pd_3Ni_7-BTP/SiO_2	nitrobenzene	ethanol	2	1	25	1	180	90	11
Pd−Ni/γ-Al_2O_3	nitrobenzene	n-hexane	1	0.41	40	H_2 flow	940.4	99.9	12
Pd@mSiO_2	nitrobenzene	ethanol	6.2	0.5	110	20	560	97	13
Pd/MIL-101	nitrobenzene	DMF	2	6	120	6	16.67	100	14
Pd/LDH nanosheets	nitrobenzene	ethanol	1	2	50	10	133.8	62.9	15
Pd-Ni-N-C_{60}	nitrobenzene	ethanol	6.71	0.5	70	10	10315	98	16
Ni-CeO_2−x/Pd	styrene	ethanol	3	0.33	25	1	6827	89	17
Pd NPs PAMAM dendrons grafted to silica polyamine	styrene	benzene	7.61	0.25	70	30	25700	100	18
C8 PdNP	styrene	chloroform	84.3	24	25	1	0.83	>99	19
Pd@chitin	styrene	methanol	1.2	1	30	50	50000	100	20

References:

1. D. Nečas, P. Klapetek, *Cent. Eur. J. Phys.* 2012, **10**, 181-188.
2. U. Cindemir, U., Z. Topalian, L. Österlund, C.-G. Granqvist, G. Niklasson, *Journal of Physics: Conference Series, IOP Publishing*, 2014, p 012012.
3. M.C. Militello, S.J. Simko, *Surface Science Spectra,* 1994**, 3**, 395-401.
4. P. Bolt, E. Ten Grotenhuis, J. Geus, F. Habraken, *Surface Science,* 1995, **329**, 227-240.
5. J.A. Rotole, P.M. Sherwood, *Surface Science Spectra,* 1998, **5**, 18-24.
6. E. Natividad, E. Lataste, M. Lahaye, J.-M. Heintz, J.-F. Silvain, *Surface Science,* 2004**, 557**,129-143.
7. T. Qi, J. Sun, X. Yang, F. Yan, J. Zuo, *Sensors,* 2019**, 19**, 3131.
8. H. Wu, L. Wang, Y. Wang, S. Guo, Z. Shen, *Journal of alloys and compounds,* 2012, **525**, 82-86.
9. J. Chastain, R. C.King Jr, *Perkin-Elmer Corporation,* 1992**, 40**, 221.
10. H. Idriss, *Surface Science*, 2021, **712**, 121894.
11. Z. Wei, D. Thushara, X. Li, Z. Zhang, Y. Liu, X. Lu, *Catalysis Communications*, 2017, **98**, 61-65.
12. Y. Jiang, Q. Li, X. Li, X. Wang, S. Dong, J. Li, L. Huo, T. Jiao, Y. Wang, F. Gao, *ACS Omega*, 2021, **6**, 9780-9790.
13. M. Lv, S. Yu, S. Liu, L. Li, H. Yu, Q. Wu, J. Pang, Y. Liu, C. Xie, Y. Liu, *Dalton Transactions*, 2019, **48**, 7015-7024.
14. X. Chen, K. Shen, D. Ding, J. Chen, T. Fan, R. Wu, Y. Li, *ACS Catalysis*, 2018, **8**, 10641-10648.
15. J. Wang, C. Du, Q. Wei, W. Shen, *Energy Fuels*, 2021, **35**, 4358-4366.
16. Y. Qu, T. Chen, G. Wang, *Applied Surface Science*, 2019, **465**, 888-894.
17. Y-F. Jiang, C.-Z. Yuan, X. Xie, X. Zhou, N. Jiang, X. Wang, M. Imran, A.-W. Xu, *ACS Applied Materials & Interfaces*, 2017, **9**, 9756-9762.
18. E. Karakhanov, A. Maximov, Y. Kardasheva, V. Semerina, A. Zolotukhina, A. Ivanov, G. Abbott, E. Rosenberg, V. Vinokurov, *ACS Applied Materials & Interfaces*, 2014, **6**, 8807-8816.
19. M. A. Mahdaly, J. S. Zhu, V. Nguyen, Y.-S. Shon, *ACS Omega*, 2019, **4**, 20819-20828.
20. X. Pei, Y. Deng, Y. Li, Y. Huang, K. Yuan, J.-F. Lee, T.-S. Chan, J. Zhou, A. Lei, L. Zhang, *Nanoscale*, 2018, **10**, 14719-14725.